Composite Action between Beams and Slabs Under Transverse Load

(1) A Slab, with Identical Spanwise Beams Repeated at Equal Intervals, supported over several Transverse Supports.

by

D. N. de G. Allen, M.A. †

and

R. T. Severn, B.Sc., Ph.D. ††

SUMMARY

The analysis of a structure composed of beams integral with a slab is properly a three dimensional problem. In this paper, the need for a three dimensional treatment is obviated by an analysis of the slab according to thin plate theory and of the beams, treated separately from the slab, by the theory of simple bending. The fact that the beams are actually integral with the slab is then recognised by enforcing displacement and strain compatibility at the slab-beam junctions. Both the stress-function, describing forces in the plane of the slab, and the transverse deflection of the slab are governed by a biharmonic equation; series solutions for these two quantities are obtained subject to typical, specified, boundary conditions and to conditions of compatibility at the slab-beam junctions. The calculation of the coefficients in the series solutions would be extremely laborious if carried out by hand-computation so that a digital computer programme has been written (for the Ferranti Pegasus Computer) by use of which the complete computation can be carried out in a few minutes; thus the effect of any prescribed variation in the parameters describing either the geometry of the structure or its loading can be quickly followed through. Details of the computer programme are given.

Further papers will deal with different arrangements of slabs and beams, and also with beams which are not necessarily of constant depth across the span. Stiffened foundation mats will also be considered.

1. In a compound structure of beams integral with a slab, under transverse load, the free bending of the beams is to some extent reduced, both by the bending of the slab and, when the neutral plane of the slab does not contain the neutral axes of the beams, by forces induced in the plane of the slab as a result of the bending. Some authors[1,2] have suggested that this restriction on free-bending of a beam can be simulated by increasing the geometric second-moment of area to some 'effective' value and that, for this purpose, it is convenient to think of the beam bending, not by itself, but in conjunction with flanges taken from the slab. Thus, by concentrating attention on the beam-bending, we arrive at the concept of 'effective width' in which a certain proportion of the slab acts, in bending, with the beam. The advantage of this artifice, if we can find the magnitude of the effective width, is that design curves, which already exist, can be used in designing the structure. A difficulty of this approach is that not only has the effective width to be calculated, but also some basis for its calculation has to be established. Such a basis of calculation could be, for example, the equality of the maximum deflection of the beam, as calculated from some more or less rigorous theory, with that calculated from simple bending theory using an effective second moment of area. An alternative basis could, similarly, be the equality of maximum stress. If the effective width can be calculated for a few values of the geometric parameters describing the structure then design curves could be drawn, for a particular loading system, from which interpolated widths could be read for other values of the geometric parameters. It should be noted that the usefulness of the effective width concept lies in the assumption that the effective width is constant along the span of the beam, and of such a magnitude as to satisfy some condition, laid down for its calculation, at possibly one point only along the span.

It is probably true to say that the need for such a concept has been felt because the amount of computation required in the rational design of a composite structure was otherwise prohibitive. When, however, a digital computer programme is available the amount of time taken in computation becomes negligible, and an accurate evaluation of deflections and stresses can be made without any need for the concept; and, moreover, it becomes possible for the designer to modify the size and shape of the structure, also the loads which it is to be called upon to carry, and to observe, almost immediately, what effect his modifications will have on deflections and stresses.

The analysis of a composite slab-beam system is really a three-dimensional problem. In this paper the three-dimensional nature of the problem is by-passed by an initial separation of the slab from the beams, analysing the former by thin-plate theory and the latter by simple bending theory. The structure is then made composite by forcing the thin-plate theory and the simple bending theory to give compatible displacements and strains at the

†Professor of Applied Mathematics, University of Sheffield.
††Lecturer in Civil Engineering, University of Bristol.

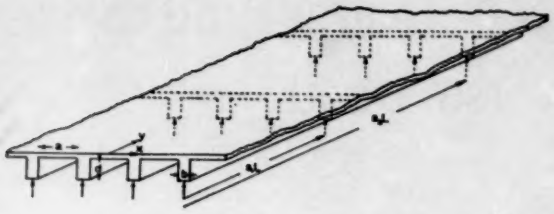

Fig. 1.

slab-beam junctions. Of course, there is some error in this process (which will be pointed out in due course) but a considerable volume of experiment[1] verifies that the error is not significant.

In the analysis which is presented here, the composite structure, which is supposed to be simply-supported at its two edges normal to the spanwise direction and to be continuous over several supports (Fig. 1), is firstly analysed under the assumption that it has no such *intermediate* supports. With the loading specified the computer programme solves the problem under this assumption and, in particular, produces values of the deflection of the beams at the positions where the intermediate supports are in reality to be provided. A second run through of the programme with unit point loads, only, acting on all the beams at one intermediate support (e.g. at $y = s_1 L$ in Fig. 1) again produces values of deflections at this and all other support points. This second step is repeated with unit point loads acting in turn at as many different support positions as exist. A linear combination of all the solutions which have thereby been obtained can then be made to produce zero deflection at all the support points. The complete sequence of operations is carried out automatically within the computer once the programme and the data have been fed into it; the final solution, printed by the machine, is that for the actual structure which is continuous over the given number of supports, simply-supported on two edges and carrying the specified loading. From the method of solution it is evident that any postulated sinking of the supports could be accounted for, as could a situation where the supports are elastic.

This paper is concerned with the general problem of the analysis of multi-span, composite structures but there are two particular cases which are of special interest. The first is the case when there are no intermediate supports; we then have a single-span structure, simply-supported at its ends. This configuration can be obtained by giving the s-values (describing the positions of intermediate supports, Fig. 1) appropriate magnitudes. The second interesting particular case is obtained by considering a structure with a number of spans, say five, which is loaded symmetrically with respect to the intermediate supports; the centre span of the five then effectively behaves as a single-span structure with its beams encastré at the edges. The slope of the slab, in the spanwise direction, is also zero at the edges, although its deflection is not forced to be zero there by the above considerations, so that we do not by this artifice quite get the solution to the problem where the whole structure (slab and beams) has encastré edges; the beams do, however, generally supply the greatest part of the resistance to bending in the spanwise direction and the fact that *they* can be made encastré means that a good approximation is achieved to the problem where the whole structure has encastré edges, the approximation becoming better as the beam spacing is reduced. To analyse a structure falling within either of the above special cases no modification to the computer programme needs to be made; it is merely necessary to arrange for the data-tape to contain appropriate essential information.

2. Fig. 1 shows the arrangement of the structure and the meaning of the symbols used. It is assumed that simple-support conditions exist on $y = 0$ and $y = L$. The beams in the structure are of rectangular cross-section, are equally spaced and, *as far as the analysis is concerned*, are infinite in number. That is to say, the analysis is strictly valid only for those parts of the structure which are uninfluenced by its termination in the x-direction. Three kinds of loading have been considered in writing the programme,
   (i) Uniformly distributed load on the slab (dead-weight or live-load),
   (ii) Uniformly distributed load along the beams, of the same intensity on each beam (dead-weight or live-load),
   (iii) Groups of point loads on all the beams, of the same value on each beam at any one spanwise position. (It is necessary to consider several such groups of point-loading).

   With these kinds of loading, model tests[1] have shown that beams two spaces from the termination in the x-direction behave as though the beams *were* repeated to infinity, and comparison with the model test results shows that our analysis is also within practical accuracy for beams one space from the termination.

3. The equations governing the plane stress-function, f, and the transverse deflection, w, are respectively

$$\left.\begin{aligned} &\nabla^4 f = 0 \\ \text{and}\quad &D\nabla^4 w = q \end{aligned}\right\} \quad \ldots\ldots\ldots \quad (1)$$

where D is the flexural rigidity of the slab and q the intensity of uniformly distributed load acting on it. Solutions to the equations (1) in the region $-a/2 \leqslant x \leqslant a/2$, $0 \leqslant y \leqslant L$, between two adjacent beams, may be taken in the form

$$\left.\begin{aligned} f = {} & \Sigma \sin \varepsilon y [A_n \cosh \varepsilon x + B_n x \sinh \varepsilon x + C_n \sinh \varepsilon x \\ & \qquad + D_n x \cosh \varepsilon x], \\ w = {} & \Sigma \sin \varepsilon y [q_n + P_n \cosh \varepsilon x + Q_n x \sinh \varepsilon x \\ & \qquad + R_n \sinh \varepsilon x + S_n x \cosh \varepsilon x], \end{aligned}\right\} \quad (2)$$

the summations extending over positive integral values of n. By virtue of the symmetry about both $x = 0$ and $y = L/2$, these reduce to

$$\left.\begin{aligned} f = {} & \Sigma \sin \varepsilon y [A_n \cosh \varepsilon x + B_n x \sinh \varepsilon x], \\ w = {} & \Sigma \sin \varepsilon y [q_n + P_n \cosh \varepsilon x + Q_n x \sinh \varepsilon x], \end{aligned}\right\} \quad (3)$$

where $\varepsilon = n\pi/L$, $q_n = 4qL^4/(n\pi)^5 D$, and the summations extend over odd positive integers n. The series (3) satisfy the necessary conditions of symmetry and also three of the four conditions of simple support on $y = 0$ and $y = L$, viz., the conditions that on these edges

(i) the deflection, $w = 0$,

(ii) the bending moment, $M_y \equiv \dfrac{\partial^2 w}{\partial x^2} + \sigma \dfrac{\partial^2 w}{\partial y^2} = 0$,

(iii) the normal stress in the plane of the slab,

$$\widehat{yy} \equiv \frac{\partial^2 f}{\partial x^2} = 0.$$

The fourth condition, which is not however satisfied, is that

(iv) the shear stress in the plane of the slab,

$$\widehat{xy} \equiv -\frac{\partial^2 f}{\partial x \, \partial y} = 0.$$

At the expense of considerable complication in the first of (3), the series form for the stress-function, this fourth edge condition can be satisfied and the solution made mathematically correct, but model tests[1] have shown that theoretical results based on (3) are, within the limits of experimental accuracy, in reasonable agreement with experimental deflection and strain measurements. Theoretical work using a series solution (other than the first of (3)) which *does* allow satisfaction of condition (iv) has also shown that little error results from using the first of (3) for the stress-function*.

*The question of the satisfaction of condition (iv) is discussed in an Appendix to this paper, where it is demonstrated that the failure of the series (3) formally to satisfy the condition is not significant.

4. The constants A_n, B_n, P_n and Q_n in the series (3) remain to be found by satisfaction of further conditions at the slab-beam junction. First, conditions of symmetry there require that

$$\left.\begin{aligned} &\frac{\partial w}{\partial x} = 0 \\ \text{and} \quad &u = 0 \end{aligned}\right\} \text{ on } x = a/2, \text{ for all } y, \quad \cdot \quad \cdot \quad (4)$$

where u is the displacement component in the x-direction. Satisfaction of the first of (4) by (3) leads to

$$P_n = -Q_n\left[\frac{1}{\varepsilon} + \frac{a}{2}\coth\frac{\varepsilon a}{2}\right]. \quad \cdot \quad \cdot \quad \cdot \quad \cdot \quad (5)$$

To satisfy the second of (4) we employ the relation $E\frac{\partial u}{\partial x} = \widehat{xx} - \sigma\widehat{yy}$, and the fact that u is zero on $x = 0$, for all y, to obtain

$$A_n = B_n\left[\frac{1-\sigma}{1+\sigma}\cdot\frac{1}{\varepsilon} - \frac{a}{2}\coth\frac{\varepsilon a}{2}\right]. \quad \cdot \quad \cdot \quad \cdot \quad (6)$$

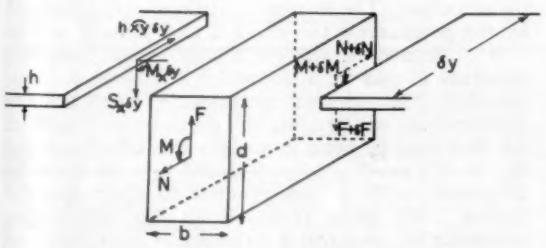

Fig. 2.

Two further relations are needed before all the constants can be computed, and these are obtained by consideration of conditions of equilibrium and of strain-compatibility at the slab-beam junction. By reference to Fig. 2, consideration of the equilibrium of a beam element (dy) gives

$$\left.\begin{aligned} &p^1 dy + dF - 2S_x dy = 0, \\ &dN - 2h\widehat{xy}dy = 0 \\ \text{and} \quad &dM + F dy - 2h\widehat{xy}l dy = 0, \end{aligned}\right\} \quad \cdot \quad \cdot \quad (7)$$

where $l = (d-h)/2$, $M = EI\frac{\partial^2 w}{\partial y^2}$

and $S_x = -D\left[\frac{\partial^3 w}{\partial x^3} + (2-\sigma)\frac{\partial^3 w}{\partial x\,\partial y^2}\right]$.

The quantity p^1, the transverse load per unit length acting on the beam element, includes both externally applied loads and the deadweight of the beam. From the first and third of (7), by elimination of F, we obtain

$$EI\frac{\partial^4 w}{\partial y^4} + 2S_x - p^1 - 2hl\frac{\partial\widehat{xy}}{\partial y} = 0. \quad \cdot \quad (8)$$

Equality of strain at the slab-beam junction gives (it being assumed that the direct force N is distributed uniformly over the beam cross-section)

$$\frac{N}{bd} + El\frac{\partial^2 w}{\partial y^2} = \widehat{yy} - \sigma\widehat{xx}. \quad \cdot \quad \cdot \quad \cdot \quad (9)$$

The second of (7), together with the fact that $N = 0$ at $y = 0$, enables us on integration to replace N in (9) by $-2h\frac{\partial f}{\partial x}$. Satisfaction of (8) and (9) by (3) then requires that

$$P_n[EI\varepsilon^2 + 2D(1-\sigma)T] + Q_n[\tfrac{1}{2}EI\varepsilon^2 aT - 2D(1+\sigma)T + D\varepsilon a(1-\sigma)] - A_n[2hl\varepsilon T] - B_n[2hlT + hl\varepsilon a] = \frac{K_n}{C\varepsilon^2} - \frac{4qEI}{LDC\varepsilon^3} + \frac{4p}{LC\varepsilon^3}, \quad \cdot \quad \cdot \quad (10)$$

and

$$P_n[El] + Q_n[\tfrac{1}{2}Elat] + A_n\left[\frac{2hT}{\varepsilon bd} + (1+\sigma)\right] + B_n\left[\frac{2hT}{\varepsilon^2 bd} + \frac{ah}{\varepsilon bd} + \frac{2}{\varepsilon} + \tfrac{1}{2}(1+\sigma)aT\right] = -\frac{4qEl}{LCD\varepsilon^5} \quad \cdot \quad \cdot \quad \cdot \quad \cdot \quad (11)$$

where $T = tanh\frac{1}{2}\varepsilon a$, $C = cosh\frac{1}{2}\varepsilon a$, p is the uniformly distributed part of p^1 and K_n is the Fourier cofficient in the expansion of the remaining part of p^1 in odd sines. In order to find P_n, Q_n, A_n and B_n for any given system of loading (symmetrical about $x = 0$ and $y = L/2$) it is necessary to solve (5), (6), (10) and (11) simultaneously for as many successive values of n as may be necessary to obtain practical convergence of the series (3). This kind of repetitive calculation is ideally suited to a digital computer and a previous programme has been written, and described elsewhere[3], for composite slab-beam structures spanning between simple supports.

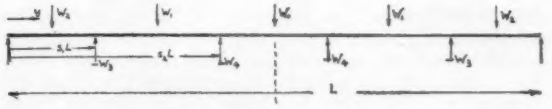

Fig. 3.

5. When the composite slab-beam structure has intermediate supports across the span, the previous analysis and computer programme would still suffice if the values of the redundant reactions at the support were known; for these reactions could then be taken into account in the terms K_n. These reactions are not known, however, but instead must be found as part of the solution. As an illustration of the computational procedure, incorporated in a new programme, consider the arrangement, shown in Fig. 3, in which there are four intermediate supports. In addition to uniformly distributed load over the slab (of area-intensity q) and uniformly distributed load along each beam (of line-intensity p)

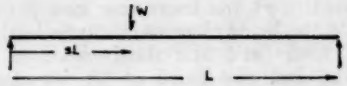

Fig. 4.

we make provision for point-loads, W_0, W_1 and W_2, acting on each beam at the centre-points of the individual spans. The redundant reactions, also shown in Fig. 3, are treated as negative loads and denoted by $-W_3$ and $-W_4$. If we consider a single point-load, W, acting on each beam of a simply-supported structure of span L at a distance sL ($0 \leqslant s \leqslant 1$), from the edge $y = 0$ (Fig. 4) it may be shown that the coefficients K_n are equal to $(2W/L)\sin ns\pi$. When all the point-loads and redundant reactions of Fig. 3 are acting the first term on the right-hand side of (10) becomes

$$2[W_0 \sin\tfrac{1}{2}n\pi + W_1\{\sin\tfrac{1}{2}n(s_1+s_2)\pi + \sin\tfrac{1}{2}n(2-s_1-s_2)\pi\} + W_2\{\sin\tfrac{1}{2}ns_1\pi + \sin\tfrac{1}{2}n(2-s_1)\pi\} + W_3\{\sin ns_1\pi + \sin n(1-s_1)\pi\} + W_4\{\sin ns_2\pi + \sin n(1-s_2)\pi\}]/LC\epsilon^2 \quad \cdot \quad (12)$$

in which, of course, the arithmetic values of W_3 and W_4, if we knew them, would be negative. If we remove the intermediate supports, that is put $W_3 = W_4 = 0$, a first run-through of the computer programme would provide values of the transverse deflections at $y = s_1L$ and $y = s_2L$ under the action of the loads q, p, W_0, W_1 and W_2; let these deflections be d and D, respectively. A second run-through of the programme with $q = p = W_0 = W_1 = W_2 = W_4 = 0$ but $W_3 = 1$ will give corresponding deflections (d' and D') due to unit, negative, support reactions at $y = s_1L$. A third run-through with $q = p = W_0 = W_1 = W_2 = W_3 = 0$ but $W_4 = 1$ will give corresponding deflections (d'' and D'') due to a unit, negative, support reaction at $y = s_2L$. If we now define α and β by

$$\left.\begin{aligned} d &= \alpha d' + \beta d'' \\ D &= \alpha D' + \beta D'' \end{aligned}\right\} \quad \cdot \quad \cdot \quad \cdot \quad \cdot \quad (13)$$

and run the computer programme through a fourth time with q, p, W_0, W_1 and W_2 taking their given values, $W_3 = -\alpha$ and $W_4 = -\beta$, the computer will obtain the solution with zero deflection at both $y = s_1L$ and $y = s_2L$ and, on account of the symmetry about $y = L/2$ which has been preserved throughout, at the other two supports as well. It is clear that any specified sinking of the supports could be accounted for in the foregoing method, as could a problem with elastic supports. The computer programme is so designed that the four runs-through described above follow automatically, in succession, after a single, original, input of the necessary data. The intermediate results, d, D, d', D', d'' and D'' are retained in the computer which also automatically solves equations (13) to obtain values for α and β.

6. Working details of the computer programme will be published elsewhere; it is sufficient here to make a few general remarks on the input of information about the structure and its loading, and on the output of results.

The input tape, for four intermediate supports, consists of the sixteen, signed, numbers

$a/2$, b, d, L, h, E, σ, q, W_0, W_1, W_2, p, s_1, s_2, W_3, W_4.

The last two numbers are not really part of the input information and are always put equal to zero, their values for the first run-through; they are included in the data-tape for subsequent ease in the organisation of the computation.

The output tape is printed as follows

Q_1
P_1
w at $y=L/2$, for $n=1$
Q_3
P_3
w at $y=L/2$, for $n=3$
...
...
...
...
Q_{15}
P_{15}
w at $y=L/2$ for $n=15$

} for p, q, W_0, W_1 and W_2 having their given values, and $W_3 = W_4 = 0$,

the twenty-four above quantities for

$p=q=W_0=W_1=W_2=W_4=0$, $W_3=1$,

the twenty-four above quantities for

$p=q=W_0=W_1=W_2=W_3=0$, $W_4=1$,

the twenty-four above quantities for p, Q, W_0, W_1, W_2 as given, and $W_3=-\alpha$, $W_4=-\beta$,

w at $y = s_1L$
w at $y = s_2L$

} for the last loading condition.

The last two quantities printed should, of course, be zero and they are included in the output as a check that the computation has been carried out correctly. The computation could be carried out up to any value of n but exploratory work has shown that, for the types of loading considered, eight terms in the series solutions is quite enough. The coefficients Q_n and P_n are printed so that, with a small amount of hand computation the transverse deflection can be calculated from (3) at any point in the structure. The transverse deflection is calculated by the programme for $y = L/2$ and printed so that if it is desired to analyse a single-span composite structure of this kind, for which the beam-ends are encastré, the present programme (without any modification) will produce the centre-span deflection. All that need be done to achieve this effect is to put $W_1 = W_2 = W_0$, $s_1 = 0{\cdot}2$ and $s_2 = 0{\cdot}4$ on the data-tape, with p and q equal to their specified values. We shall then obtain the centre-span deflection for an encastré structure of span $L/5$ under uniformly distributed load on the slab, uniformly distributed load along the beams and a point load (W_0) at the centre-span of all beams.

7. As an illustration of the use of the programme we consider a single-span composite structure and investigate the difference, in the centre-span deflection, between conditions of simple support and conditions of fixity of the beam-ends. For this purpose we consider two different specimens whose geometry is defined as follows:

	$a/2$	b	d	L	h	E	σ
Specimen 1	3·625	0·375	0·9	29·0	0·15	4777·0	0·3
Specimen 2	6·0	0·375	0·9	24·0	0·15	4777·0	0·3

All dimensions are in inches and E in tons/in^2. For Specimen 1 loading conditions are taken as $p = q = 0$

with W, the point-load at the centre-span position of each beam, as 60 lb. For Specimen 2, $W = 0$, $p = 0{\cdot}723$ lb/in. and $q = 1{\cdot}922$ lb/in^2. Such specimens, with the loads quoted, have been studied experimentally[1] and measurements made of the mid-span deflections (w_a) of the centre beam of such structures with five beams composite with the slab when the edges were simply supported. In these experiments the model structure was built up from aluminium sheet and bar, and the beams cemented to the slab with araldite resin. From subsidiary experiments it was found that this method of construction did reproduce the conditions assumed in the theoretical work up to the intensity of loading to be used. The point-loads, which were applied to the centre-span point of each beam, were transmitted by a system of levers from dead-weight loading pans located on either side of the model. The uniformly distributed load was produced by compressing an air-bag between the model and a thick steel plate. The air-bag could not, in fact, be made to cover the very corners of the model without overhanging in other parts but that this system did produce an effective uniformly distributed load was proved by applying it first to a thin slab with stiffening beams and comparing experimental deflections with those which had been calculated from accepted theories. Calculations have also been made, using the earlier computer programme[3] to obtain those deflections (w_b), again for the case of simply supported edges. We now use the computer programme which is the subject of this paper to calculate the mid-span deflection (w_c), when conditions of end-fixity apply, for the same specimens and applied loads. In order to do this, the data-tape must be punched with the information in the table* following, the first line being for Specimen 1 and the second line for Specimen 2.

*In this table the loads are quoted in ton units.

$a/2$	b	d	L	h	E	σ	q
3·625	0·375	0·9	145·0	0·15	4777·0	0·3	0
6·0	0·375	0·9	120·0	0·15	4777·0	0·3	0·00086
W_0	W_1	W_2	p	s_1	s_2	W_3	W_4
0·02679	0·02679	0·02679	0	0·2	0·4	0	0
0	0	0	0·00032	0·2	0·4	0	0

The results are collected and compared in the following table, the entries being in inches $\times 10^{-3}$:

	w_a	w_b	w_c
Specimen 1	51	47	14
Specimen 2	66	64	38

The small discrepancy between w_a and w_b for specimen 1 can be attributed, in some degree, to experimental error and also in part to assumptions made in the theoretical work (such as the assumption that the direct force N is uniformly distributed across the beam cross-section). The effect of fixing the beam-ends against rotation is to produce a considerable reduction in the value of the deflection although, for these specimens, the beam spacing is large in relation to the other dimensions.

8. The computer programme described in this paper deals with four intermediate supports, symmetrically disposed about $y = L/2$, but it can be immediately applied, by suitable punching on the data-tape, to problems where there are no intermediate supports at all. If there is an even number of intermediate supports greater than four, or if there is an odd number of intermediate supports, again symmetrically disposed about $y = L/2$, a small modification to the programme as at present written would be necessary.

The time taken for computation on one set of data is approximately three minutes, which means that possible alternative values of parameters can be followed through in a very short time.

REFERENCES

1. Holmes, M., *Ph.D. Thesis* (University of Bristol, 1958).
2. Odquist, F., "On the effective width of reinforced plane plates" (*Royal Swedish Air Board*, Translation No. 5, 1948).
3. Severn, R. T., "Composite action between beams and slab under transverse load using the Pegasus Computer" (*C. & C.A. Specification for Digital Computers*, 1960).

APPENDIX

The series form for the stress-function, the first of (3), has been shown to satisfy all the necessary conditions except the one requiring $\widehat{xy}$ to be zero on the simply-supported edges of the slab. The analysis in the body of the paper is mathematically lacking to this extent, but it has been assumed that no significant error would arise on this account; the validity of this assumption is supported by the agreement between our results and those of a considerable body of experiment[1]. We now derive an alternative, more complicated, series-form for the stress-function, f, in order that a theoretical test of the assumption can be imposed. It is convenient to change the origin of coordinates (Fig. 1) to the point $x = 0$, $y = L/2$. It can be then verified that the series

$$f = \Sigma_r[A_r \cosh\varepsilon x + B_r x \sinh\varepsilon x]\cos\varepsilon y + \Sigma_n C_n[\tfrac{1}{2}L \sinh\tfrac{1}{2}\alpha L \cosh\alpha y - y \sinh\alpha y \cosh\tfrac{1}{2}\alpha L]\cos\alpha x \quad \cdots \quad (14)$$

where $\varepsilon = r\pi/L$, $\alpha = n\pi/a$, and the summations extend over odd integral values of r and n respectively, satisfies all the conditions which (3) had satisfied and, by virtue of the introduction of the C_n terms, also allows $\widehat{xy}$ to be made zero on the simply-supported edges, $y = \pm L/2$. The corresponding series form for the transverse deflection is

$$w = \Sigma[q_r + P_r \cosh\varepsilon x + Q_r x \sinh\varepsilon x]\cos\varepsilon y$$

where $q_r = 4qL^4 \sin\tfrac{1}{2}r\pi/(r\pi)^5 D$.

For $\widehat{xy}$ to be zero on $y = \pm L/2$, for all x, we obtain

$$\Sigma_n C_n \alpha[\tfrac{1}{2}\alpha L + \cosh\tfrac{1}{2}\alpha L \sinh\tfrac{1}{2}\alpha L]\sin\alpha x = \Sigma_r[B_r\varepsilon(\sinh\varepsilon x + \varepsilon x \cosh\varepsilon x) + A_r\varepsilon^2 \sinh\varepsilon x]\sin\tfrac{1}{2}r\pi \quad \cdot \quad (15)$$

In order to find the coefficients C_n from (15) it is necessary to expand both $\sinh\varepsilon x$ and $x\cosh\varepsilon x$, on the right hand side, in odd sine series (of $\sin\alpha x$). If the double summation on the right-hand side of (15) is then re-arranged we obtain equations of the form

$$C_n = \Sigma_r \beta_{rn} A_r + \Sigma_r \gamma_{rn} B_r$$

for each value of n.

When the C_n terms were absent the four coefficients A_r, B_r, P_r and Q_r could be calculated for $r = 1$ and the calculation repeated in turn for $r = 3, 5, 7, \ldots$, for as many values of r as were found necessary, each group of four constants being calculated separately; in fact, we had a system of four simultaneous equations to solve for each value of r. The effect of the inclusion

of the C_n terms is to make all the constants interdependent. Thus, if we wish to calculate k terms of the series, we have to solve, not k independent sets each of four equations, but instead one set of $5k$ simultaneous equations. The magnitude of such a computation using hand calculating machines is formidable but for reasonable values of k it presents no difficulty when a digital computer is employed.

In the absence of the C_n terms the equations (5), (6), (10) and (11) expressed satisfaction of various conditions for all values of y and it was from these four equations that we were able to calculate the values of the constants. The inclusion of the C_n terms modifies all but one of these equations by the inclusion of functions of y such as $\cosh\alpha y$ and $y\sinh\alpha y$. Before the equations can now be satisfied for all y it is necessary to expand $\cosh\alpha y$ and $y\sinh\alpha y$ in odd cosine series (of $\cos\varepsilon y$). For example, the corresponding form of (6) is

$$\Sigma_r\Big[\Big\{B_r(1-\sigma)-A_r\varepsilon(1+\sigma)\Big\}\sinh\tfrac{1}{2}\varepsilon a - \tfrac{1}{2}(1+\sigma)B_r\varepsilon a\cosh\tfrac{1}{2}\varepsilon a\Big]\cos\varepsilon y + \Sigma_n C_n \sin\tfrac{1}{2}n\pi\Big[\Big\{\tfrac{1}{2}(1+\sigma)\alpha L\sinh\tfrac{1}{2}\alpha L - 2\cosh\tfrac{1}{2}\alpha L\Big\}\cosh\alpha y - \Big\{(1+\sigma)\alpha\cosh\tfrac{1}{2}\alpha L\Big\}y\sinh\alpha y\Big] = 0, \quad (16)$$

and we find that

$$\cosh\alpha y = \Sigma_r\left\{\frac{4a^2r}{\pi(n^2L^2+a^2r^2)}\sin\frac{r\pi}{2}\cosh\frac{\alpha L}{2}\right\}\cos\varepsilon y \quad (17)$$

$$y\sinh\alpha y = \Sigma_r\left[\frac{2Lra^2}{\pi(n^2L^2+a^2r^2)}\sin\frac{r\pi}{2}\left\{\sinh\frac{\alpha L}{2} - \frac{4Lan}{\pi(n^2L^2+a^2r^2)}\cosh\frac{\alpha L}{2}\right\}\right]\cos\varepsilon y. \quad (18)$$

If we let the quantities in curled brackets, in (17) and (18) respectively, be represented by I and II then (16) becomes

$$A_r[-\varepsilon\sinh\tfrac{1}{2}\varepsilon a] + B_r\left[\frac{1-\sigma}{1+\sigma}\sinh\tfrac{1}{2}\varepsilon a - \tfrac{1}{2}\varepsilon a\cosh\tfrac{1}{2}\varepsilon a\right] + \Sigma_n C_n \sin\tfrac{1}{2}n\pi\left[\left\{\tfrac{1}{2}\alpha L\sinh\tfrac{1}{2}\alpha L - \frac{2}{1+\sigma}\cosh\tfrac{1}{2}\alpha L\right\}I - \left\{\alpha\cosh\tfrac{1}{2}\alpha L\right\}II\right] = 0.$$

The equations corresponding to (10) and (11) can be obtained in a similar manner. Equation (5) is unaffected by the inclusion of the C_n terms.

The experimental and theoretical work mentioned in the body of the paper suggests that the inclusion of the C_n terms will make no appreciable difference to the results obtained and that, because of this, the simple theory can be used with confidence. To check this suggestion a digital computer programme has been written which includes the C_n terms and the computation has been carried out on data for which the solution by the simpler theory had previously been obtained by another programme[3]. The problem is that of a single-span composite structure of a slab and beams simply supported along the two edges normal to the spanwise direction and loaded equally at the centre-span points of all beams. The coefficients which were obtained with, and without, C_n terms are collected in the table below: It is clear that the inclusion of the C_n terms does not make any practically significant difference to the values of the coefficients.

Discussion

The Council would be glad to consider the publication of correspondence in connection with the above paper. Communications on this subject intended for publication should be forwarded to reach the Institution by August, 31st, 1961.

	P_1	Q_1	A_1	B_1	C_1
C_n terms not included.	46·069	−2·443	6278·19	−1328·83	—
C_n terms included.	46·212	−2·441	6312·62	−1351·52	−0·001886
	P_3	Q_3	A_3	B_3	C_3
C_n terms not included.	−0·598	0·080	−87·72	32·16	—
C_n terms included.	−0·577	0·077	−57·57	25·18	$-0{\cdot}00021\times 2^{-38}$

Wind Structure and the Assessment of Wind Loads

by Walter A. Woeber, D.Sc., M.I.Mech.E., M.(S.A.)I.C.E.

1. Introduction

Structural analysis devolves upon two essential operations: the assessment of the external forces to which a structure may be subjected, and the determination of the internal stresses induced by these forces in the various portions of a structure.

In specifying the external forces, recourse is usually had to accepted codes of practice which recommend the loading to be taken into account for a variety of conditions. It is not sufficiently realised, however, that these load classifications are of necessity imperfect representations of actual conditions. This arbitrariness is particularly evident in the case of the design wind loads laid down in building codes.

The purpose of this paper is to bring the problems associated with the assessment of wind loads in the design of exposed engineering structures within the purview of that part of dynamical meteorology which deals with atmospheric motion near the ground.

2. Atmospheric Turbulence

Atmospheric motion, which becomes apparent to the observer as wind, is generally of a very complicated nature. The term 'wind' is restricted to the horizontal component of this motion and is specified by its speed and the direction from which it blows. Wind speed and direction are subject to rather wide and rapid fluctuations and exact specification or mathematical analysis is difficult.

The motion of the atmosphere, particularly in the surface layers, is usually turbulent. Firstly, there is the mechanical effect of irregularities on the ground, giving rise to frictional eddies which are carried along with the wind. Secondly, owing to the heating of the air at the earth's surface, convectional eddies are set up and develop freely when the heating is intense.

Dry air, when heated by contact with a warmer ground surface, rises and expands and cools adiabatically at the rate of 1°C in 100m. This is known as the adiabatic lapse rate.

By day, the atmospheric temperature gradient may exceed the adiabatic lapse rate and facilitate the formation of turbulence. The thermal currents due to convection may either form part of the general turbulence or appear as small travelling eddies caused by local temperature differences on the ground, where bare soil, rock or sand absorb the incoming solar radiation more readily than grasslands, wooded areas or water surfaces.

By night, when the ground is cooled by the flow of the outgoing radiation, the air tends to attain the same temperature as the ground with which it is in contact and the lapse rate may become inverted or isothermal through a layer of 500 ft. or more. An inversion is characterised by its pronounced stability which damps out convection and prevents turbulent mixing.

The degree of turbulence which may be present in the atmosphere at any time is clearly demonstrated by the trail of smoke from a chimney. Disregarding for the purpose of this discussion, the force of buoyancy of hot plumes and the topographic effect on plume dispersion, the shapes traced out in a fresh breeze will assume distinct patterns which can readily be associated with the various temperature lapse rates, as shown in Fig. 1.

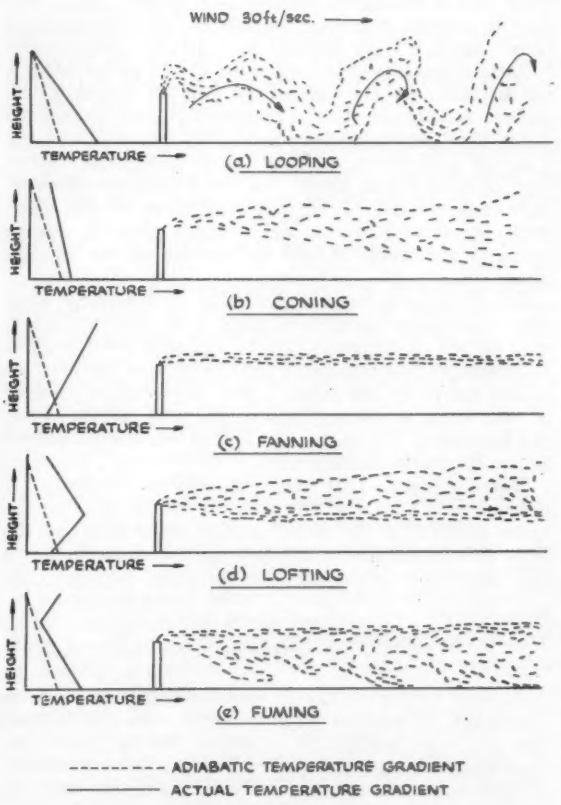

Fig. 1.

The variation of atmospheric temperature with height is shown diagrammatically on the left hand side of Fig. 1 for each of the five cases (a) to (e) illustrated. The adiabatic lapse rate has also been plotted to serve as a comparator.

In 1 (a) the lapse rate is clearly super-adiabatic and the marked thermal turbulence resulting therefrom is demonstrated by the 'looping' of the smoke emission.

Temperature conditions approximating to the dry-adiabatic lapse rates are represented in 1 (b), and the resulting smoke plume is in the form of a horizontal cone.

A temperature inversion in the atmosphere, 1 (c), denotes thermal stability, illustrated by the almost laminar flow from the stack which is referred to as 'fanning.'

Conditions associated with an inversion near the ground and a super-adiabatic gradient above it, are shown in 1 (d). The thinning out owing to convection from the top of the otherwise laminar emission has been termed 'lofting.'

Finally, in 1 (e), super-adiabatic conditions exist near the ground and an inversion above the top of the stack. Rising of the smoke is prevented by the stable conditions at the upper level; the smoke stratifies and forms a screen below which atmospheric turbulence causes 'fuming' or the spreading downwards of the smoke. This is the condition responsible for the formation of what has popularly been termed 'smog.'

Steady or streamline motion is a rather exceptional case in nature and even the almost laminar emission shown in Fig. 1 (c) appears as a steady motion only to the human observer who looks at the plume from a far distance. In the case of the laminar emission, the radius of the circular cross-section containing 90 per cent of the suspended smoke particles will be about $\frac{1}{2}$ in. at a distance of 30 ft. from the point source (top of stack), and about 5 in. at a distance 3,000 ft. further downwind. In an unsteady wind the turbulent exchange is of a much higher order and the smoke spreads out very much faster, as shown in the illustrations.

The transition from a steady to an unsteady wind motion has its parallel in fluid flow through pipes, well known to engineers, where a change from laminar to turbulent flow depends upon the ratio of the product of the radius of the pipe, r, and the average velocity of the fluid, u, to a physical property of the fluid, the kinematic viscosity, ν. The ratio, u/ν, is known as the Reynolds number (Re).

Remembering that the kinematic viscosity is defined as the ratio of the absolute viscosity, μ, to the mass density of the fluid, ρ, the importance of the Reynolds number becomes immediately apparent from the following relationship:

$$ur/\nu \propto \tfrac{1}{2}\rho u^2/(\mu u/r) \propto \frac{\text{dynamic force}}{\text{viscous force}} \quad . \quad . \quad . \quad (1)$$

At low values of the Reynolds number the flow is controlled by viscous forces, disturbances are damped out and the motion is steady. When this ratio increases, the dynamic forces become more powerful, disturbances are not so easily damped out and the flow breaks down into a violent eddying.

The analogy of pipe flow is, however, relatively simple when compared with atmospheric motion and it is not possible to apply the Reynolds number in a straightforward manner to problems connected with the flow of the natural gusty wind.

When considering atmospheric motion, the dimension r is presumably to be taken to measure the height of the homogeneous air mass at the observing station, so that motion on such a vast scale must be turbulent even at relatively low wind speeds. Only during an inversion or with air motion corresponding to light winds up to force 3 on the Beaufort scale (5 m/sec) is the flow nearly laminar.

The above considerations show clearly that the state of the atmospheric motion is not specified by the Reynolds number alone but that account must also be taken of the prevailing temperature gradient. Conditions of zero lapse rate, as they occur in a wind tunnel, make the interpretation of laboratory tests a matter of considerable difficulty. The wind speed and viscosity are the same in the wind tunnel and in the atmosphere, so that the Reynolds number in the test is reduced by the scale of the model. In practice there is, however, a vast difference between the two Reynolds numbers which clearly indicates that the simulated flow in the wind tunnel is far from being dynamically similar to the atmospheric motion.

A criterion for deciding whether steady or unsteady conditions exist in the atmosphere and, further, whether atmospheric turbulence will subside or increase, has been enunciated by *L. F. Richardson*[1] whose work in this respect is comparable to that of Osborne Reynolds. For the purpose of this paper the Richardson number (Ri) may be stated as follows:

$$Ri = \frac{g}{\tau}\left(\frac{d\tau}{dz} + \gamma\right) \Big/ \left(\frac{du}{dz}\right)^2 \quad . \quad . \quad . \quad (2)$$

where u = average wind velocity,
z = height above the ground,
g = acceleration of gravity,
τ = temperature at level z,
γ = adiabatic lapse rate,
$d\tau/dz$ = observed temperature gradient,
du/dz = velocity gradient.

The critical value of this parameter, below which turbulence sets in, and above which conditions tend to become vertically stable, has been estimated by Richardson at unity. Although other investigations have thrown some doubt on the validity of $Ri_{\text{crit}} = 1$, work carried out by *C. S. Durst*[2] in the lower layers of the atmosphere has shown that there is ample evidence to support Richardson's criterion.

3. Wind Structure and Gustiness

From the foregoing it is clear that the motion of the atmosphere is not constant, neither in space nor in time; wind speed and direction vary continually. If these variations take place at definite intervals and reach definite amplitudes, they are referred to as gusts.

The gustiness of the wind is defined by the passage of a quantity of air (M) across a control surface (A):

$$M = \int_A \rho\, u \cos\alpha \, d\sigma \quad . \quad . \quad . \quad . \quad . \quad (3)$$

where ρ = air density,
u = wind velocity,
α = angle of incidence of wind direction,

$\int d\sigma = A$ = area of the control surface.

Depending upon whether u, α, ρ, or A varies, the above expression permits distinctions to be made between sudden fluctuations of wind speed, direction, density or the cross-sectional area of the wind stream. In the present paper attention will be focused on the speed and directional variations of the wind as recorded by a pressure-tube anemometer.

The pressure-tube anemometer was designed by W. H. Dines, F.R.S., when, after the Tay Bridge disaster in 1879, special attention was devoted to the measurement of gusts. The instrument is based on the principle of the Pitot-tube and is kept pointed into the wind by means of a vane. The static tube is vertical. The wind blowing into the impact tube produces an increase of pressure inside it which is transmitted through the central supporting tube to the recording apparatus. The central tube is surrounded by an outer tube in which there are four rows of holes to provide a suction effect. The difference between the pressure and the suction effect is made to actuate a float or diaphragm whose motion is recorded by a pen on a chart.

The trace of the pressure-tube anemometer affords information as to the internal structure of the wind. The width of the trace is an indication of the degree of gustiness, and it is usually possible to insert, by eye, a mean line through such a trace and so to determine the mean wind at any time.

A closer examination of an anemometer trace reveals that periods of stronger and weaker fluctuations alternate so that the record assumes the character of a stepped profile. This is more clearly brought out in the enlarged reproduction of a recorded wind gust, shown in Fig. 2, which was obtained by increasing the speed of the drum recorder.

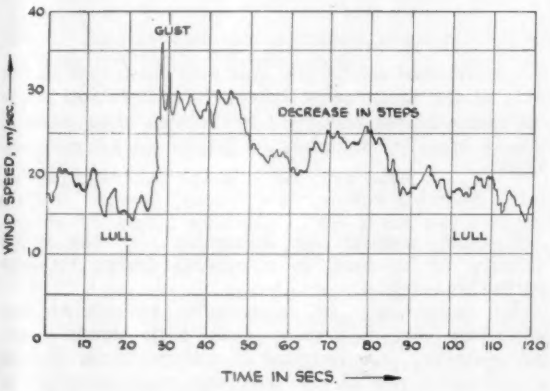

Fig. 2.

The short fluctuations, with periods of a few seconds only, are caused by surface friction ; superimposed on these and characterised by comparatively wide fluctuations are disturbances with periods of several minutes. The latter are caused by thermal eddies and are largely responsible for the gusts and lulls in the wind motion.

The basic character of the record of a gust is nearly always the same : after a steep rise, the wind speed dies down in gradual steps, the gust is followed by a lull. Although it might appear that a mean line drawn through the succession of irregularities follows a sine oscillation with a decreasing amplitude, the numerous errors in geometrical form preclude the evaluation of anemograms by the methods of analytical geometry. It is however possible to apply the impulse theorem to the irregular atmospheric motion.

As stated above, the mean line through an anemometer trace can usually be determined with sufficient accuracy by eye. For a relatively short time interval, represented by the ' sampling length ' of the mean line, the mean velocity can be stated for any point on the curve. If the mean values of the components of the wind motion, referred to the rectangular co-ordinate system in space, are denoted by $\bar{u}$, $\bar{v}$, and $\bar{w}$, and the temporary deviations from the mean by u', v', and w', then the actual wind velocities at any particular time are

$$u = \bar{u} + u',\ v = \bar{v} + v',\ w = \bar{w} + w'.$$

In applying the impulse principle to wind motion, it is not sufficient to apply it to the average motion ; the mean value must be obtained from the individual impulses passing through the fixed control surface (A), referred to earlier. In what follows, the u-component only of the wind motion will be considered.

During the time interval dt, a mass $\rho\, u dt$ passes through the control surface with the velocity u. The impulse for the time dt is therefore $\rho\, u^2 dt$. The total effect over a longer period of Time T is

$$\frac{1}{T}\int_0^T \rho\, u^2\, dt \text{ per second.}$$

Using the notation previously adopted, namely placing a bar above the symbols to denote mean values, the above expression may be written in the form $\rho\, \overline{u^2}$. Now $u^2 = (\bar{u} + u')^2 = (\bar{u})^2 + 2\,\bar{u}\,u' + (u')^2$ . . (4)

In forming the mean value of u^2, written $\overline{u^2}$, it must be borne in mind that $\bar{u}$ already represents the mean value of u ; further, the mean value of u' is zero by definition, but this does not apply to mean values of squares of u' Hence

$$\rho\, \overline{u^2} = \rho\, (\bar{u})^2 + \rho\overline{(u')^2} \quad . \quad . \quad . \quad . \quad . \quad (5)$$

Thus, the total effect is obtained by adding to the impulse of the average motion the impulse resulting from the mean value of the square of the deviations.

4. Evaluation of Anemograms

The force on an object submerged in a fluid stream depends upon the shape, the size, the velocity of the flow, the density of the fluid, and the viscosity.

By the application of the principles of dimensional analysis, the relationship may be expressed as follows :

$$F = \tfrac{1}{2}\,\rho u^2 l^2\, \varphi \quad . \quad . \quad . \quad . \quad . \quad . \quad (6)$$

where F = fluid force,
ρ = mass density of the fluid,
u = velocity of flow,
l = typical dimension of the submerged object,
φ = a function of the Reynolds number.

The factor $\frac{1}{2}$ has been inserted in equation (6) because $\frac{1}{2}\rho u^2$ has a physical significance as the pressure which would result from a complete conversion of the kinetic energy of the wind into its pressure equivalent. Since, in the case of wind motion, the Reynolds number is largely influenced by the thermal stratification of the atmosphere, φ is, in a sense, a function of a function. The degree of gustiness present in the atmosphere at any time is, however, reflected by the width of the anemometer trace so that, in the evaluation of wind records, due cognisance is taken of Reynolds' and Richardson's parameters.

As l is a linear dimension which defines the shape of the submerged object, l^2 may be replaced by A, its projected area on a plane perpendicular to the fluid force. In order to allow for the different resistances to the air flow which arise from the particular shapes of the objects exposed to the wind stream, the term A, for the projected area, is grouped with a shape factor, S. This coefficient has widely different values for bodies of different shape and is lowest for streamlined objects.

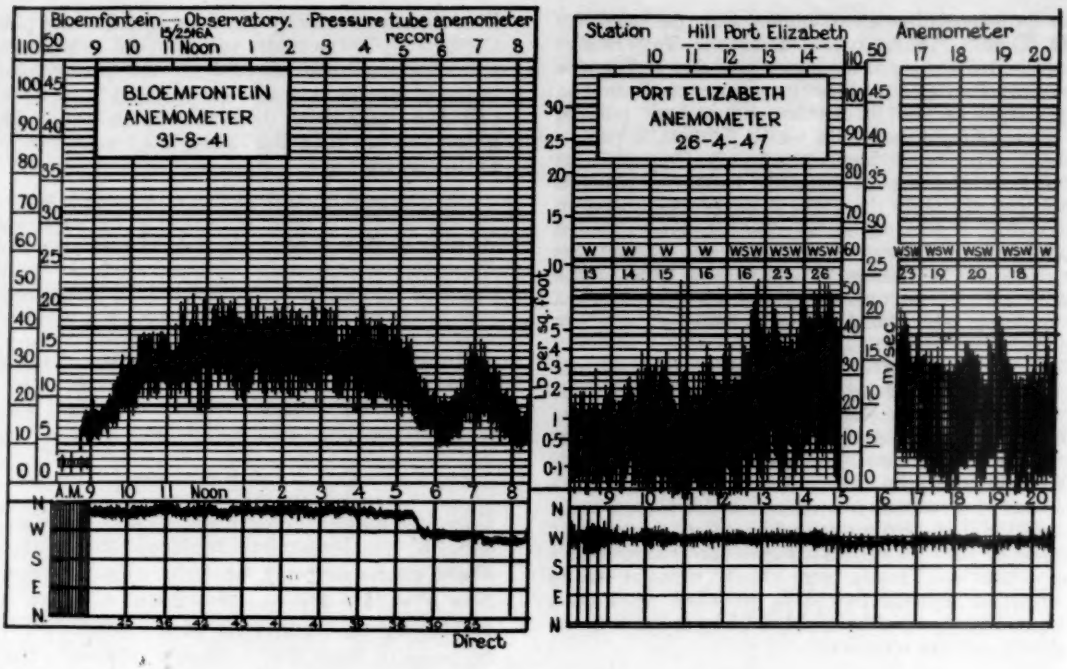

Fig. 3.

In wind pressure calculations, where the shape of a structure exposed to the wind is unusual and available data are insufficient, recourse must be had to wind tunnel experiments to assign a value to the shape coefficient. The variation of the shape factor with the Reynolds number, the so-called 'scale effect,' is fortunately not appreciable in the case of engineering structures, which generally have sharp edges or corners so that the shape coefficients obtained under simulated flow conditions may be accepted, albeit with caution as previously emphasised.

By taking ρ to be 0·00238, its value at 15°C and 760 mm. Hg., and expressing the wind velocity in miles per hour, U, equation (6) may be written in the following form :

$$F = 0{\cdot}0026\, SAU^2 \qquad \cdot \quad \cdot \quad \cdot \quad \cdot \quad (7)$$

In order to allow for the racking action of the pulsating wind force, the design wind velocity, U, is grouped with a gustiness coefficient, G, so that the wind pressure formula to be applied in structural design may be stated as follows :

$$P = 0{\cdot}0026\, SGU^2 \qquad \cdot \quad \cdot \quad \cdot \quad \cdot \quad (8)$$

where $P = F/A$ = wind pressure intensity in lb/ft.^{2}.

The gustiness coefficient plays a somewhat analogous part to that which the coefficient of impact plays in structural design to denote the number by which the computed static stress is multiplied to obtain the value of the increased stress assumed to be caused by the suddenness of application of the live load.

The degree of gustiness is indicated by the width of the trace of a recording pressure-tube anemometer, as shown in Fig. 3, which has been chosen to illustrate two cases of extreme gustiness recorded at the Bloemfontein and Port Elizabeth aerological stations.

S.P. Wing[3] recommends an increase of 25 per cent of the readings taken with a cup anemometer.

W. A. Woeber[4] relates the gustiness coefficient to the ratio of the mean amplitude of the valleys and peaks traced by the recording pen to the highest mean wind over a specified sampling length of an anemogram. Thus

$$G = 1 + \overline{u'}/\overline{u} \qquad \cdot \quad \cdot \quad \cdot \quad \cdot \quad \cdot \quad (9)$$

It now remains to determine U, the wind velocity to be used in structural design for any particular locality.

An examination of anemometer records at any observing station reveals that high winds occur infrequently ; it is essential, therefore, to use as long a period as possible in selecting an anemogram of extreme wind conditions for the purpose of evaluation. The record so selected should in fact represent the wind extremes over a period of not less than twenty years.

Exhaustive investigations by *W. Schmidt*[5] have shown that, strictly speaking, wind records are valid only for the immediate neighbourhood of the aerological station at which they were taken, and that there is no ready method of obtaining representative data for larger districts from the extreme values so determined. It is therefore necessary to analyse the wind records and to specify the maximum intensities for a number of well distributed aerological stations and thereby divide a district into regions according to their respective windiness. A survey of this nature has been carried out by *W. A. Woeber*[6] for the Union of South Africa.

Since the anemograms selected for analysis record exclusively the horizontal component of the wind motion, the following considerations will be confined to the u-component of this motion. It is clear that the total wind effect which must be accounted for in structural design is equal to the sum of the effects due to the mean wind and the fluctuations about the

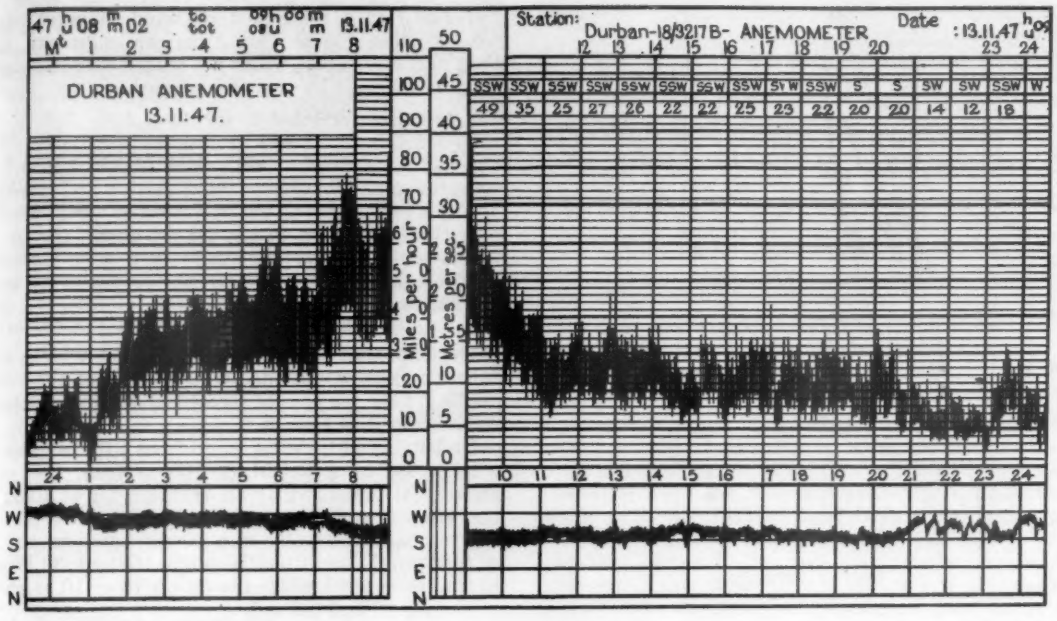
DURBAN ANEMOMETER
13.11.47.
Station: Durban-18/3217B- ANEMOMETER Date : 13.11.47
Miles per hour
Metres per sec.
SSW SSW SSW SSW SSW SSW SSW SW SSW S S SW SW SSW W
49 35 25 27 26 22 22 25 23 22 20 20 14 12 18
N W S E N

Fig. 4.

mean. In accepting this argument, equation (5) may be re-written in the following form :

$$\rho \overline{u^2} = \rho U^2 = \rho(\bar{u}^2 + \overline{u'^2}) \quad \cdot \quad \cdot \quad \cdot \quad (10)$$

Thus, the two principal quantities to be obtained from the anemogram are $\bar{u}$, the 'highest mean,' and $\overline{u'}$, the mean value of the deviations.

The 'highest mean' is entered on the wind record simply by visual estimate as the mean value of the maximum and minimum speeds over a sampling length representing one hour.

The corresponding record of the deviations from the mean speed over the same sampling length forms, owing to the slow rotation of the instrument drum and the thick trace of the recording pen, a more or less irregular jagged area which is determined by the use of a planimeter. Division of this area by the scale length of one hour then yields an approximate value of the mean amplitude of the deviations.

5. Practical Application

In order to demonstrate the method evolved for the determination of the 'design wind' for any particular area, the following example will be helpful.

On the 13th November, 1947, the City of Durban experienced a wind storm which caused structural damage estimated at well above £100,000. Only once in Durban's previous recorded history, namely in May, 1905, did the wind reach similar gale force. The anemogram, recorded at the Durban Meteorological Office, is shown in Fig. 4.

It will be seen that the wind rose at about midnight and at 2 o'clock was blowing from WSW with an average speed of 30 mph and gusts up to 44 mph, increasing steadily to an average of 40 mph with gusts up to 64 mph at 7 o'clock.

At 7.45 a.m., the wind veered to SW and averaged 59 mph for nearly half an hour, registering occasional gusts up to 78 mph.

From 8.55 to 9.10 a.m. the gale blew southerly with a sustained fury of 62 mph and gusting up to 88 mph ; thereafter the wind dropped steadily until evening, when increasing heavy falls of rain marked its dying violence.

The period of maximum wind speed and deviations over a sampling length of one hour is indicated in the enlarged section of the anemogram shown in Fig. 5.

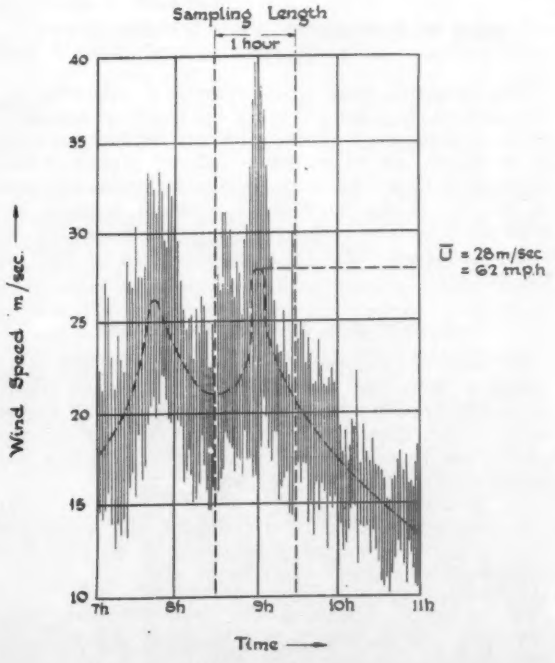

Fig. 5.

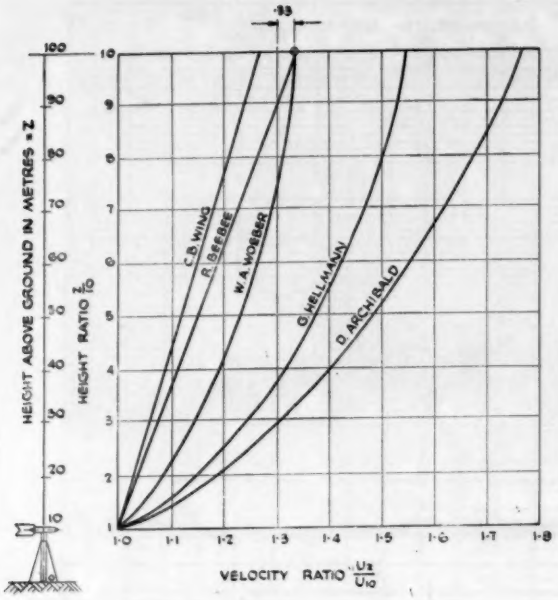

Fig. 6.

It will be noted that the insertion by eye of the 'mean line' presents no difficulty. For the portion of the anemogram represented by the sampling length. the evaluation yields :

Highest Mean	$= \overline{u}$	$= 62$ mph
Mean Deviation	$= \overline{u'}$	$= 27$ mph
Design Wind	$= U_{10}$	$= (62^2 + 27^2)^{1/2}$ $= 67{\cdot}6$ mph
Gustiness Coefficient	$= G$	$= 1 + 27/62$ $= 1{\cdot}43$
Basic Wind Pressure	$= p$	$= 0{\cdot}0026\, G\, U^2$ $= 17$ lb/ft.^{2}

The estimated basic wind pressure, p, refers to the design wind, U_{10}, computed for the height of exposure of the anemometer nozzle, which is normally placed at a height of 10 m (33 ft.) above ground level. Depending upon the shape of the structure exposed to the wind, the basic wind pressure, p, must be multiplied by the respective shape coefficient, S, in order to obtain the wind pressure, P, to be used in the design.

6. Variation of Wind with Height

A factor of great practical importance in structural design is the increase of wind pressure with the height above the ground. Observations of the flow of liquids in pipes have shown that in turbulent flow the velocity profile can be represented by a fractional power law of the distance from the pipe wall :

$$u = z^{1/x} \quad \cdot \quad \cdot \quad \cdot \quad \cdot \quad \cdot \quad \cdot \quad (11)$$

Experiments which fitted the fractional power law were made by *Douglas Archibald* with anemometers suspended from kites up to 1,300 ft. above the ground ; they resulted in the formula :

$$U_z/U_{10} = (z/10)^{0{\cdot}25} \quad \cdot \quad \cdot \quad \cdot \quad \cdot \quad (12)$$

In this and the following expressions, the velocities U_z and U_{10} occur at heights z and 10 m above the ground level.

J. Feld,[8] in a discussion on wind pressure, quotes two formulae due to two American engineers, C. B. Wing and R. Beebee, which are stated below, using the notation adopted by the present author :

$$U_z/U_{10} = 1 + 0{\cdot}003\,(z - 10) \quad \cdot \quad \cdot \quad \cdot \quad \cdot \quad (13)$$

and

$$U_z/U_{10} = 1 + 0{\cdot}004(z - 10) - 0{\cdot}000003(z - 10)^2 \quad \cdot \quad (14)$$

On the analogy between wind motion and river flow, *G. Hellman*[9] expressed the variation of wind speed as a logarithmic function of the height above the ground, similar to the method employed in hydraulic engineering for the calculation of the stream velocities at various depths, namely :

$$U_z/U_{10} = 0{\cdot}233 + 0{\cdot}656\, log\,(z + 4{\cdot}75) \quad \cdot \quad (15)$$

The exponent of the power function which, in the author's view, would adequately represent the velocity profile for the purpose of structural design calculations, is determined as follows :

Under extreme wind conditions, the increase of wind speed at a height of 100 m from the ground above that measured by an anemometer at 10 m from the ground is found to be only about 33 per cent. Plotted logarithmically as a power function, the slope of the straight line from the origin to the 1·33 intercept at the 100 m level, where the ratio $z/10 = 10$, is given by

$$log\ 10/log 1{\cdot}33 = 8$$

which represents therefore the exponent of the function

$$z/10 = (U_z/U_{10})^8 \quad \cdot \quad \cdot \quad \cdot \quad \cdot \quad \cdot \quad (16)$$

This relationship is more suitably written in the transposed form :

$$U_z/U_{10} = (z/10)^{0{\cdot}125} \quad \cdot \quad \cdot \quad \cdot \quad \cdot \quad (17)$$

The various formulae which have been put forward to express the variation of wind with height, are plotted in Fig. 6.

The values of the coefficients in Hellman's formula and the powers in the interpolation formulae, are influenced largely by the coefficient of roughness of the ground surface and even more so by the degree of turbulence present in the atmosphere. From the surface up to a level beyond the influence of surface friction the wind backs and increases in speed at a rate depending upon the atmospheric turbulence.

At about 1,500 ft. level the motion of the air is free from the effect of surface friction and is maintained by the balance of the forces due to the earth's rotation and to the pressure gradient. The momentum of the surface wind is less than that of the upper wind, but owing to turbulence there is a tendency towards equalisation.

The structural engineer is mainly concerned with wind extremes, when the turbulence level in the atmosphere is high and the vertical transport of momentum is rapid, so that the wind velocity measured at the height of the anemometer nozzle approximates more closely to that of the upper wind.

From the above considerations it is reasonable to infer that, where monthly and annual averages of upper winds are required, the velocity profiles corresponding to the Hellman and Archibald formulae will serve. For structural engineering purposes, however, the steeper curves plotted in the diagram, Fig. 6, should be considered when adopting a height factor, $H = U_z/U_{10}$, by which the design wind at 10 m must be multiplied in order to obtain the design wind for the required level.

7. Wind-Excited Oscillations

An engineering structure possess a period of vibration which depends upon its mass. The gustiness of the wind constitutes a periodic force whose period may

agree with the natural period of the structure upon which it acts. These vibrations are accompanied by stresses set up in the structure. When the period of the gust is in resonance with the natural period of the structure, the amplitude of the resulting motion is much larger than that which occurs when the two periods differ. Consequently the stresses induced in the structure are increased and may rise beyond the elastic limit. The collapse, in 1940, of the suspension bridge over the Tacoma Narrows in Washington is one of the most spectacular failures of this nature.

The frequency of vibration due to a wind stream is directly proportional to the velocity of the wind. Taking the simple case of an overhead transmission line, the induced frequency, f_1, is given by

$$f_1 = k.v/d \quad \cdots \quad (18)$$

where

k = Strouhal number, presently to be discussed,
v = wind speed, and
d = diameter of the cable.

The natural frequency, f_n, of the overhead line may be represented by

$$f_n = \frac{1}{2s}\sqrt{\frac{T}{m}} \quad \cdots \quad (19)$$

where

s = distance between nodes,
T = tension, and
m = mass of unit length,

so that in the event of resonance, when $f_1 = f_n$, the vibrations set up attain to dangerous proportions.

Even in steady winds, rapid vibrations of small amplitude which lead to breaks in cable strands are possible due to eddies which form behind obstructions such as insulators and tower members, provided the wind remains steady long enough for the vibration to be set up by resonance.

Vibrations of transmission lines of large amplitude are known as whipping, galloping or dancing. The period of these vibrations has been estimated at about 3 seconds, mainly from the cinematographic records of the Hydro-electric Power Commission of Ontario.

The galloping of transmission lines is generally associated with glaze storms, and the primary cause of these large vibrations may be attributed to a deposit of ice on the lee side. The wire, having lost its circularity of section, acquires a self-exciting characteristic which, drawing energy from the wind, stimulates vibrations of a cumulative character.

Wind-excited vibrations have also been observed on tall, self-supporting steel stacks. As in the case of overhead high tension cables, a stack exposed to the wind stream will give rise to the generation of eddies on the leeward side. These eddies develop alternately on opposite sides of the stack transverse to the wind direction and are carried down-wind, forming a double row of evenly spaced staggered vortices, as shown in Fig. 7.

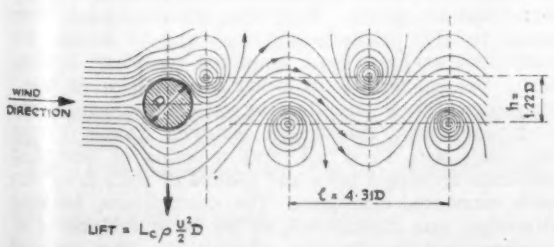

Fig. 7.

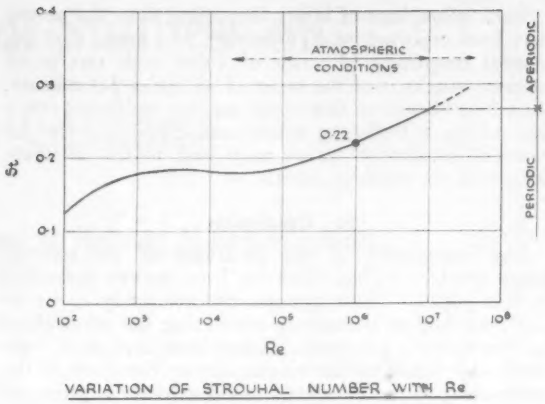

VARIATION OF STROUHAL NUMBER WITH Re

Fig. 8.

A criterion for the stability of a vortex trail has been enunciated by *Th. von Kàrmàn*[10] who found that in most cases the vortices shed from the cylinder faded away rapidly and that only for a definite ratio of the distance between the two eddy paths, h, and the spacing of the eddies in a single path, l, did the trail persist over an appreciable distance :

$$h/l = 0{\cdot}283 \quad \cdots \quad (20)$$

The generation of the vortices is associated with a change in the circulation around the stack which gives rise to a lift or lateral force alternating at a frequency equal to that of eddy formation, namely

$$Lift = L_c \rho \frac{u^2}{2} D \quad \cdots \quad (21)$$

where

D = diameter of the stack

and

L_c = lift coefficient, which is assumed to vary as a simple harmonic function.

Experimental values for L_c, quoted by *R. Ruedy*[11] vary from 0·61 to 1·05.

The frequency of eddy formation, f, is given by Equ. (18) and may be re-stated in the following form

$$f = St.\, v/D \quad \cdots \quad (22)$$

where

D = diameter of the stack,

and

$St = fD/v$ = a dimensionless ratio, called the Strouhal number, after *V. Strouhal*[12], the first investigator of this phenomenon.

Although the Strouhal number for bluff bodies with sharp edges or corners is little affected by atmospheric turbulence, this is not so in the case of cylindrical objects, as demonstrated by the curve of Fig. 8.

For atmospheric conditions with Reynolds numbers below 10^7, a mean value of $St = 0{\cdot}22$ may be used in the calculation of the frequency with which the vortices are shed. For values of Re approaching 10^7, atmospheric turbulence reaches a level of intensity at which the generation of vortices ceases to be periodic.

It is clear, therefore, that extreme conditions of atmospheric motion and turbulence are less conducive to setting up periodic transverse forces which may coincide with the natural frequency of the stack. This is borne out by the failure of a welded stack of 16 ft. diameter and 300 ft. height, reported by *Den Hartog*[13], which came to resonance at its natural frequency of about 1 cycle per second in a wind of less than 50 miles per hour.

Stack vibrations of lower frequency than the above have been reported by *K. Döring*[14], who found that the natural frequency of sway of 100*m* high reinforced concrete stacks is of the order of 25 cycles per minute. Gust frequencies of this order are not unlikely; they can set up a buffeting action and cause a period of resonant oscillation which may lead to the ultimate fatigue of the stack materials.

8. Conclusion

The complexity of the structure of the natural gusty wind is evident from the brief survey presented in this paper. There appears unfortunately to be no short method of accurately estimating the wind effect for engineering purposes. It has been said that " the ideal way would be for the engineer to obtain from the meteorologist the maximum wind velocity a proposed structure should be able to withstand and how often that velocity would be expected to occur."

The author's method of assessing wind extremes for engineering purposes merely extends the routine evaluation of anemograms at meteorological stations, but it is hoped that it may help to discourage the use of arbitrary rules in the design of exposed engineering structures. Many problems which need further investigation suggest themselves from the paper.

Finally, the author wishes to make acknowledgement to the British Electrical and Allied Industries Research Association (E.R.A.) for permission to publish this paper.

References

1. Richardson, L. F., *Phil. Mag.*, 49, 1925.
2. Durst, C. S., *Journ. Roy. Met. Soc.*, Vol. LIX, 1933.
3. Wing, S. P., *Report* 31, *Struct. Div., Proc. ASCE*, 1932.
4. Woeber, W. A., *Zeitschr. Ing. & Arch. Verein, Heft* 7/8 *Vol.* 95, Vienna, 1950.
5. Schmidt, W., *Probleme der Kosm. Physik*, 7, Hamburg, 1925.
6. Woeber, W. A., *Thesis, Tech. Univ.* Vienna, 1948.
7. Douglas Archibald, E., *Nature, Vol.* 33, 1886.
8. Feld, J., *Journ. Franklin Inst.*, May 1945, p. 368.
9. Hellman, G. *Meteorol. Zeitschr.*, 1917, p. 273.
10. von Karman, Th., *Nachr. d. Ges. d. Wiss*, Goettingen, 1911-12.
11. Ruedy, R., *Canadian Journ. of Research*, Oct., 1935.
12. Strouhal, V., *Annalen der Physik, Vol.* 5, 1878.
13. Den Hartog, J. P., *Proc. Nat. Acad. Sc. of U.S.A., Vol.* 40, *No.* 3, 1954.
14. Döring, K., *Der Bauingenieur*, 1924, p. 547.
15. General Reference, Brunt, D. A., *Physical and Dynamical Meteorology*, Cambridge, 1939.

Discussion

The Council would be glad to consider the publication of correspondence in connection with the above paper. Communications on this subject intended for publication should be forwarded to reach the Institution by August 31st, 1961.

Book Reviews

Calcul Rapide des Poutres Continues, by M. M. Marcel and Andre Reimbert. (Paris : Edition Eyrolles, 1960). 260 pp. 8½ in. × 6 in. approx. Price 340 N.F. plus postage 35·45 N.F.

The original theorem of three moments may now not be used generally so much in this country, owing to the advent of newer alternative methods. However, the three moment theorem is fundamental and has many applications and uses of its own and cannot be dispensed with. On the other hand, the method is often long and tedious, so that an approximate, but sufficiently accurate, variation to ease the work and reduce the time in the solution of cases is always welcome.

This book, compiled and written by two French Consulting Engineers, goes thoroughly and deeply into cases that arise under uniform and point loads on series of varying spans. It can confidently be recommended to French-reading engineers for use in solving their problems.

The method follows the rule enunciated by M. Caquot, whence, by simple substitutions, the results obtained give satisfactory solutions confirmed by tests on reinforced concrete beams and slabs.

The rule is clearly explained in the pages following the Preface by M. V. Bollard, who states that it is the best and simplest method for these calculations, and he compliments the authors on their important work of direct application, and for their derivations of formulae for spans up to four and more in number under different loadings.

The mathematics are clear and sufficient, while the 157 tables, charts and diagrams are adequate and give all the essentials required for design. Moreover, in worked examples the final application to the design of reinforcement is also given.

L.T.

Reinforced Concrete Piling and Piled Structures, 2nd Edition, by F. E. Wentworth-Sheilds, W. S. Gray and H. W. Evans. (London : Concrete Publications, 1960). 9 in. × 6 in. 149 pp. 18s.

The second edition of this book contains in a concise form much information for designers, constructional engineers, and students concerned with the manufacture, driving, and design of precast concrete piles, the testing of soils, and the design of piled structures. The design data is in accordance with the latest British codes of practice, and examples of methods of design and construction, and illustrations of many structures are given. Extensive revisions have been made to the previous edition, subjects which are additional or have been amplified including loading tests, the calculation of bearing capacities of piles, the design of sheet-pile retaining walls, and specifications and quantities. The stresses occurring during driving are dealt with in detail, and methods of designing pile-caps for single piles and groups of piles are given with numerical examples. The descriptions, working drawings, and illustrations of works in the course of construction, justify the addition to the title of " Piled structures."

On the Torsional Stiffness of Box Section Girders*

by F. Laszlo,† Dr. Ing. (Darmstadt) and H. Nolle,†† M.Eng.Sc. (Melb.)

SYNOPSIS

The behaviour of a structural member subjected to a torsional load may be defined by its torsional rigidity and the stress distribution over its cross section. As distinct from the solid or hollow cross section which is homogeneous in the axial direction, the semi-closed box section represents a three-dimensioned problem of a complex nature. This Paper attempts a solution by the Strain Energy method leading to expressions of torsional rigidity of a particular type of design and also analyses the stress distribution, the results being expressed in terms of the applied torque.

Considering these factors, a method has been devised of designing such girders subjected to combined bending and torsion within the elastic range.

An experimental programme has been carried out on full scale girders subjected to pure torsion and results were found in general to be in agreement with the theoretical work.

NOTATION

A_c	cross sectional area of channel
A_r	cross sectional area of bracing rod
A_p	cross sectional area of end plate
C	torsional rigidity
D	distance between centres of channels
D_1	distance between intersections of centre lines of bracing rods
E	Young's Modulus
G	Shear Modulus
H	overall width of channel
I	moment of inertia of bracing rod
I_y, I_z	moment of inertia of channel about y, z axes
I_{max}, I_{min}	moment of inertia of end plate about principal axes
L	length of bay
P	force causing torque
Q, S	shear force
R	moment arm
T	applied torque
U	strain energy
V	shear force
W	height of channel
a	developed length of channel strip
b	distance between bracing rods
b_p	width of end plate
c	thickness of channel strip
c_p	thickness of end plate
d_r	diameter of bracing rod
$e = \frac{1}{2}(D_1 - D)$	
l_b	equivalent length of bracing rod
ψ	angle of inclination of bracing rod to axis of girder
φ	angle of twist
θ	angle of twist per unit length
μ	Poisson's ratio.

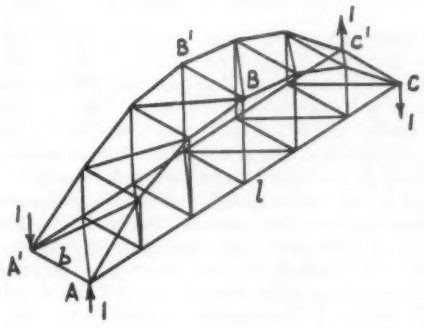

Fig. 1.

1. Introduction

One of the problems met in the design of steel structures has been quite often the determination of their elastic torsional rigidity. This has been the question not only in cases where members are subjected to externally applied twisting moments but also in problems connected with lateral buckling in bending.

Perhaps the first to give a solution to the above problem for a framed structure was Batho[1], who developed a formula for the shear in a structure subjected to torsion. For unit loads applied to the four corners (Fig. 1), the expression for panel shear was given by

$$S = \frac{bl}{2\ (area\ ABC)} \quad . \quad . \quad . \quad . \quad . \quad . \quad (1)$$

The main shortcomings of this theorem were that even though the stresses in the members of the lateral system are given directly by (1), to find those in the main truss members, additional analytical or graphical methods had to be applied. Also, the theorem assumed the ends of all members to be ball-jointed and subjected to tension or compression only.

*This paper is based on part of the thesis submitted by one of the authors (H. Nolle) for the degree of Master of Engineering Science at the Engineering School of the University of Melbourne.

†Engineering School, University of Melbourne.

††Atomic Energy Commission, Research Establishment, Lucas Height, N.S.W., Australia.

The latter deficiency is not serious when the ratios of bending and torsional resistances to length of member are small, but in certain cases for more compact sections such as considered in this Paper, effects due to bending and twisting of members have to be included.

A similar problem, but in a different field, arose in the early 1920's with the advent of the aeroplane. It concerned itself in particular with the fuselage subjected to torsional loads. Analytical methods of solution were developed by several workers[2,3], all of which, however, involved the second limitation mentioned above.

During more recent years the trend has been towards lighter construction of structural frames. Among other innovations, efforts have been made to replace heavy rolled sections by fabricated sections of light weight. The shape of such sections is manifold, but a number of these may be grouped under what is now accepted as the thin walled fabricated box section.

The Paper develops solutions to one of the problems of stress analysis of such semi-closed box sections, namely their torsional stiffness. Solutions are given as to its stiffness, strength and load capacity when the section is subjected to pure torsion.

An experimental programme on full scale girders showed good agreement with the theory developed.

2. Method of Analysis

The type of section under consideration is made up of two channels braced on the sides by continuous bent rods, the nodes of which are welded to the inside flanges of the channels as shown in Fig. 2. The ends of the girder are fitted with plates welded to the ends of the channels. Such a girder, subjected to twist, represents a statically manifold indeterminate structure. For low values of torque the strain energy of the whole girder may be expressed as a quadratic function of the forces and moments involved. Since the statically indeterminate forces and moments are all internal ones, their correct values must make the strain energy a minimum according to the Least Energy Theorem. Thus, the partial derivatives of the strain energy U of the whole girder with respect to every statically indeterminate moment and force must become simultaneously zero. This leads to as many linear equations as there are statically indeterminate forces and moments, from which the value of all statically indeterminate unknowns is obtained.

The angle of twist of the girder as a whole is obtained by Castigliano's Theorem and hence the torsional rigidity.

A convenient approach is to replace the finite girder as shown in Fig. 2 by n bays of an infinite girder of similar shape and by a finite girder having only one bay and with ends as shown in Fig. 2.

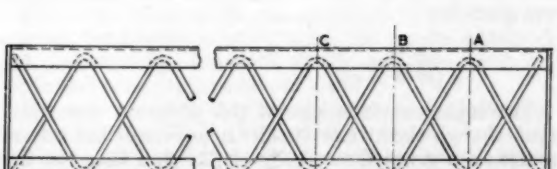

Fig. 2.

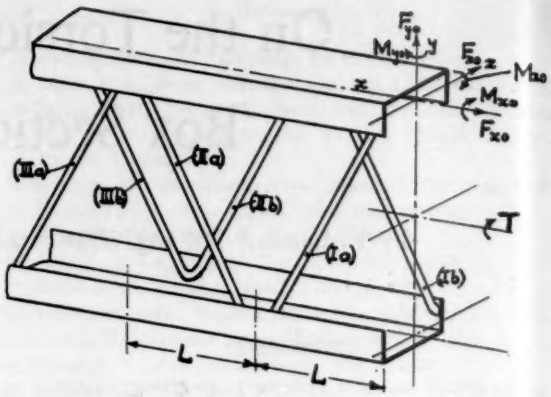

Fig. 3.

To find the strain energy of the infinite girder, that of one pitch, i.e. that of section AC is to be expressed. Though some stiffening is caused by the welds between channel and bracing at sections A, B and C, it is assumed that over an elementary length Δx at A, B and C only the channels transmit the external torque.

Let the girder be intersected at AA, and the infinite section to the right of AA be replaced by forces and moments F_{xo}, F_{yo}, F_{zo}, M_{xo}, M_{yo}, and M_{zo} applied to each of the cuts across the two channels as in Fig. 3. Next the two bracing rods *Ia* and *Ib* are separated at their junctions with the channels and forces and moments F_b, F_{bt}, F_{bz}, M_b, M_{bt} and M_{bz} applied as shown in Fig. 4.

The elementary length Δx of the two channels take over all duties at BB. For the length BC the rods *IIa* and *IIb* take their share in the torque. Separating the rods from the channels as before, the rods are now considered to be subjected to end forces and moments F_b', F'_{bt}, F'_{bz}, M'_b, M'_{bt} and M'_{bz} as in Fig. 5.

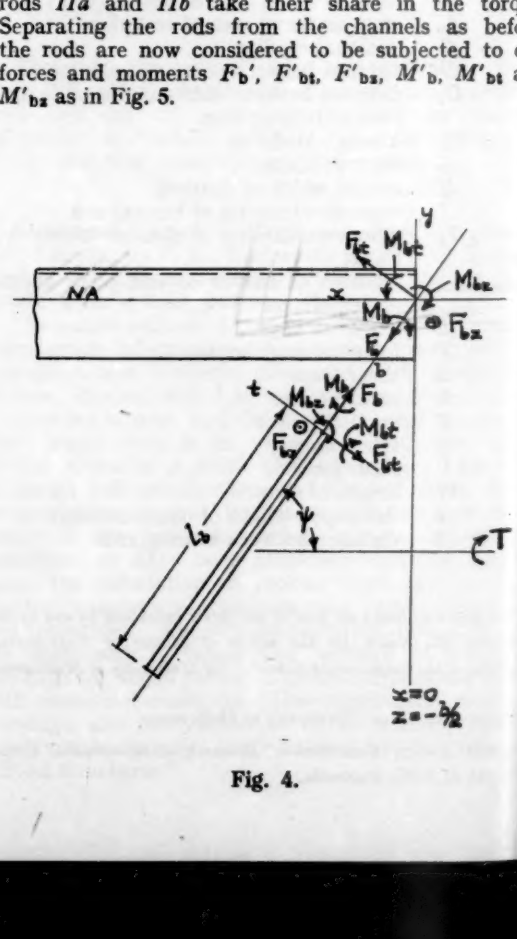

Fig. 4.

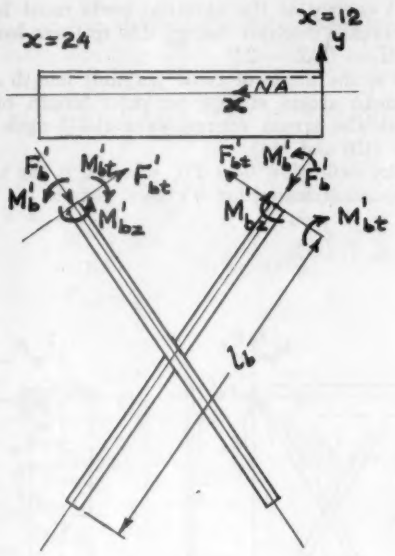

Fig. 5.

Expressing the strain energy of one pitch and differentiating it with respect to the external torque T, we obtain

$$\frac{\partial U_{AC}}{\partial T} = \varphi_{AC}$$

and

$$C_{AC} = \frac{2LT}{\varphi_{AC}}$$

where $2L$ denotes the length of one pitch.

The angle of twist is obtained in a similar fashion for the girder having one bay only. Denoting the total strain energy of channels, rods and end plates by U_E, we find

$$\frac{\partial U_E}{\partial T} = \varphi_E$$

and

$$C_E = \frac{LT}{\varphi_E}$$

Consider the twisting angle φ of the whole girder of length $(n+1)L$ due to T, viz.

$$\varphi = \frac{nLT}{C_{AC}} + \frac{LT}{C_E} = \frac{(n+1)LT}{C}$$

from which

$$C = \frac{(n+1)C_{AC}C_E}{C_{AC} + nC_E} \quad \cdot \quad \cdot \quad \cdot \quad (3)$$

2.1. *Equivalent Length of Rod*

For the purpose of analysis an equivalent length l_b of straight rod replaces the continuous bent rod. Two definitions for this length of rod may be considered.

(i) *Equal Volume*—This defines the length of the ideal straight rod as such as to make the volumes of the bent rod and that of the straight rod equal.

(ii) *Length of Centre Line*—The equivalent rod is extended to the points where the centre lines of adjacent rods intersect.

In engineering practice the second definition is generally accepted; however, solutions by both will be given for the purpose of comparison.

3. The Girder of Infinite Length

It has been shown[7] that adjacent bays do have a similar stress distribution at corresponding points, viz. $|X_{11}| = |X_{12}|$ where X_{11} and X_{12} are unknowns for the first and second bay, respectively. Thus the problem reduces to the solution of any bay along the length of the girder.

The equilibrium equations of rods, and channel of appropriate periodic length, give

$$F_{bz} = 0 \quad \cdot \quad \cdot \quad \cdot \quad \cdot \quad \cdot \quad \cdot \quad (4)$$

$$F_{xo} = 0 \quad \cdot \quad \cdot \quad \cdot \quad \cdot \quad \cdot \quad \cdot \quad (5)$$

$$F_{yo} = F_b \sin\psi - F_{bt}\cos\psi \quad \cdot \quad \cdot \quad \cdot \quad (6)$$

$$M_{bz} = \tfrac{1}{2} l_b F_{bt} \quad \cdot \quad \cdot \quad \cdot \quad \cdot \quad \cdot \quad (7)$$

$$M_{xo} = \frac{T}{2} - \frac{D}{2} F_{zo} \quad \cdot \quad \cdot \quad \cdot \quad \cdot \quad (8)$$

$$LF_{zo} = 2M_{bt}\cos\psi - 2M_b \sin\psi + F_b b \cos\psi + F_{bt} b \sin\psi \quad \cdot \quad \cdot \quad \cdot \quad \cdot \quad \cdot \quad (9)$$

3.1 *Strain Energy*

In the evaluation of half the strain energy per bay of length L we have to account for all direct acting loads as well as bending and twisting moments and shear forces. Localized stresses and stress concentrations and their effects are neglected, and the channel will be considered to be subjected to loads acting on its cross section as a whole.

The bending and tension strain energies are found in the conventional way.

The shear strain energies are for channel[4]

$$U_{F_{zo}} = \frac{9(1+\mu)L}{8EHc} F_{zo}^2 \quad \cdot \quad \cdot \quad \cdot \quad \cdot \quad (10)$$

due to F_{zo}.

Furthermore, the resolutes of rod forces F_b and F_{bt} in the x-direction act on both flanges of the channel section and in opposite direction. Replacing the concentrated reactions at the panel points by a uniformly distributed shear force Q as shown in Fig. 6 we have

$$Q = \frac{1}{L}(F_b \cos\psi + F_{bt}\sin\psi)$$

It may be shown by means of the membrane analogy[5] that the strain energy of a channel of length L is given by

$$U_Q = \frac{HQ^2L}{8cG}$$

substituting for Q and G, obtain

$$U_Q = \frac{H(1+\mu)}{4cLE}(F_b \cos\psi + F_{bt}\sin\psi)^2 \quad \cdot \quad \cdot \quad \cdot \quad \cdot \quad (11)$$

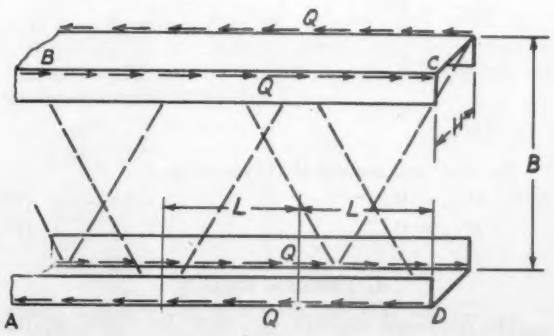

Fig. 6.

The only shear strain energy in the bracing rod[4] is due to F_{bt}, viz.

$$U_{F_{bt}} = \frac{4(1+\mu)l_b}{3A_rE} F_{bt}^2 \quad . \quad . \quad . \quad . \quad (12)$$

Denoting the total strain energies of the channel and rod by U_1 and U_2, respectively we have

$$U_1 = \frac{L}{2A_cE}\left[-F_b\cos\psi - F_{bt}\sin\psi\right]^2 + \frac{3(1+\mu)L}{ac^3E}\left[\frac{T}{2} - \frac{D}{2}F_{zo} - M_b\cos\psi - M_{bt}\sin\psi - F_b\frac{b}{2}\sin\psi + F_{bt}\frac{b}{2}\cos\psi\right]^2 + \frac{1}{2EI_y}\int_0^L\left[M_{yo} - M_b\sin\psi + M_{bt}\cos\psi + F_b\frac{b}{2}\cos\psi + F_{bt}\frac{b}{2}\sin\psi - xF_{zo}\right]^2 dx + \frac{L}{2EI_z}\left[M_{zo} + F_{bt}\left(\frac{l_b}{2} - e\sin\psi\right) - F_b(e\cos\psi)\right]^2 + \frac{9(1+\mu)L}{8EHc}F_{zo}^2 + \frac{(1+\mu)H}{4EcL}\left[F_b\cos\psi + F_{bt}\sin\psi\right]^2 \quad . \quad (13)$$

and

$$U_2 = \frac{l_b}{2A_rE}F_b^2 + \frac{(1+\mu)l_bM_b^2}{2EI} + \frac{1}{2EI}\int_0^{l_b}\left[F_{bt}\left(\frac{l_b}{2} - \xi\right)\right]^2 d\xi + \frac{l_b}{2EI}M_{bt}^2 + \frac{4(1+\mu)l_b}{3A_rE}F_{bt}^2 \quad . \quad . \quad . \quad . \quad (14)$$

The total strain energy $U = U_1 + U_2$ as given above is that of a girder length of $L/2$. Remembering that $F_{zo} = f(F_b, F_{bt}, M_b, M_{bt})$ a solution is given by the partial derivatives of U with respect to the statically indeterminate quantities equated to zero,

$$\left.\begin{aligned}\frac{\partial U}{\partial M_{yo}} &= 0\\ \frac{\partial U}{\partial M_{zo}} &= 0\\ \frac{\partial U}{\partial F_b} &= 0\\ \frac{\partial U}{\partial F_{bt}} &= 0\\ \frac{\partial U}{\partial M_b} &= 0\\ \frac{\partial U}{\partial M_{bt}} &= 0\end{aligned}\right\} \quad . \quad . \quad . \quad . \quad . \quad (15)$$

The first and second of (15) lead to

$$M_{yo} = 0 \quad . \quad . \quad . \quad . \quad (16)$$

$$M_{zo} = 0 \quad . \quad . \quad . \quad . \quad (17)$$

4. Torsional Rigidity C

The torsional rigidity can now be found by the principle of conservation of energy of the system as a whole. For an elastic system, the decrease in potential energy of the external loads must be equal to the increase in strain energy due to these loads

$$\tfrac{1}{2}T\theta L = U_oL = 2U$$

where θ is the angle of twist per unit length and U_o is the mean strain energy per unit length of girder and U is the strain energy over the length $L/2$ as given by (13) and (14).

Also, by definition $\theta = T/C$ where C is the torsional rigidity; substituting for θ above, obtain

$$\frac{C}{E} = \frac{LT^2}{4UE} \quad . \quad . \quad . \quad . \quad (18)$$

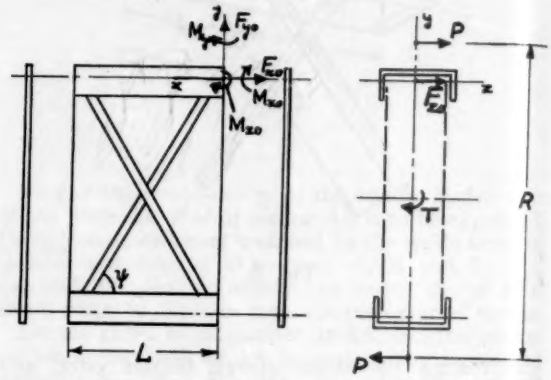

Fig. 7.

5. The Girder of Finite Length

The solution of the finite length girder follows the same line as that of the infinite girder. Figs. 7 and 8 show the coordinate system of a one-bay girder with solid end plates welded to the channels. Both plates have been separated from the channel ends and the tentatively assumed direction of torque and internal moments and forces between plate and channel are indicated. The sense of the forces and moments between bracing rods and channel bear the same relationship to the sense of the externally applied torque as in the infinite girder.

Applying the conditions of equilibrium, the following equations are obtained :—

$$F_{bz} = 0 \quad . \quad . \quad . \quad . \quad (19)$$

$$F_{xo} = 0 \quad . \quad . \quad . \quad . \quad (20)$$

$$M_{xo} = \frac{T}{2} - \frac{D}{2}F_{zo} \quad . \quad . \quad . \quad . \quad (21)$$

$$F_{yo} = F_b\sin\psi - F_{bt}\cos\psi \quad . \quad . \quad . \quad (22)$$

$$M_{bz} = \frac{l_b}{2}F_{bt} \quad . \quad . \quad . \quad . \quad (23)$$

$$M_{yo} = \frac{L}{2}F_{zo} - F_b\frac{b}{2}\cos\psi - F_{bt}\frac{b}{2}\sin\psi + M_b\sin\psi - M_{bt}\cos\psi \quad . \quad . \quad . \quad (24)$$

5.1 *Strain Energy*

The strain energy expression of one channel is slightly modified and reads now

$$U_1 = \frac{L}{2A_cE}(-F_b\cos\psi - F_{bt}\sin\psi)^2 + \frac{3(1+\mu)L}{ac^3E}\left(\frac{T}{2} - \frac{D}{2}F_{zo} + F_{bt}\frac{b}{2}\cos\psi\right.$$

$$- F_b \frac{b}{2} \sin\psi - M_b \cos\psi - M_{bt} \sin\psi \Big)^2$$

$$+ \frac{1}{2EI_y} \int_0^L \left(\frac{L}{2} - x\right)^2 F_{zo}^2 dx + \frac{L}{2EI_z}$$

$$\left[M_{zo} + F_{bt}\left(\frac{l_b}{2} - e \sin\psi\right) - F_b e \cos\psi\right]^2$$

$$+ \frac{9(1+\mu)L}{8EHc} F_{zo}^2 + \frac{(1+\mu)H}{4EcL} (F_b \cos\psi + F_{bt} \sin\psi)^2 \quad . \quad . \quad . \quad . \quad (25)$$

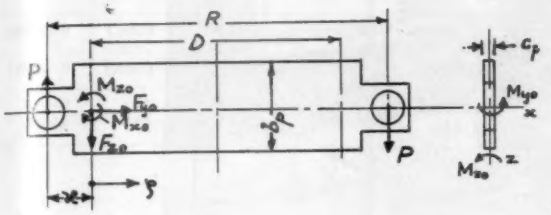

Fig. 8.

The strain energy expression of the rod is again the same as before, i.e. equation (14).

The total strain energy of the plate will be a function of the external torque T and its mode of application. One way of applying a torque is shown in Fig. 8 where $T = P.R$, and conforms with the loading of the experimental specimens.

Using the same method as before, the shear strain energy in the plate due to shear force Q is given by

$$U_Q = \frac{(1+\mu)HB}{4Ec_pL^2} (F_b \cos\psi + F_{bt} \sin\psi)^2 \quad . \quad . \quad . \quad . \quad (26)$$

Thus the strain energy U_3 of the plate becomes

$$U_3 = \frac{D}{2A_oE} \left(F_b \sin\psi - F_{bt} \cos\psi\right)^2$$

$$+ \frac{9(1+\mu)D}{8A_oE} \left(\frac{T}{R} - F_{zo}\right)^2$$

$$+ \frac{3(1+\mu)D}{b_pc_p^3E} \left(\frac{L}{2} F_{zo} - F_b \frac{b}{2} \cos\psi\right.$$

$$\left. - F_{bt} \frac{b}{2} \sin\psi\right.$$

$$\left. + M_b \sin\psi - M_{bt} \cos\psi\right)^2 + \frac{D}{2EI_{min}} M_{zo}^2$$

$$+ \frac{1}{EI_{max}} \int_0^{D/2} \left[\frac{T}{2} - \left(\frac{D}{2} - \rho\right) F_{zo}\right.$$

$$\left. - \frac{T}{R} (\rho + x)\right]^2 d\rho$$

$$+ \frac{(1+\mu)HB}{4Ec_pL^2} (F_b \cos\psi + F_{bt} \sin\psi)^2 \quad . \quad . \quad . \quad . \quad (27)$$

Now the total strain energy U of length $L/2$ of the girder is given by the sum of equation (14) (25) and (27) and the simultaneous solution of the partial derivatives of U with respect to the statically indeterminate quantities equated to zero leads to the remaining unknowns. Thus

$$\left.\begin{aligned} \frac{\partial U}{\partial F_b} &= 0 \\ \frac{\partial U}{\partial F_{bt}} &= 0 \\ \frac{\partial U}{\partial M_b} &= 0 \\ \frac{\partial U}{\partial M_{bt}} &= 0 \\ \frac{\partial U}{\partial M_{zo}} &= 0 \\ \frac{\partial U}{\partial F_{zo}} &= 0 \end{aligned}\right\} \quad . \quad . \quad . \quad . \quad . \quad (28)$$

The torsional rigidity is given by (18) after evaluating U.

It may be noted that the solution of the latter type i.e. one for a single bay girder may be used to compare experimental and theoretical results directly without the help of equation (3), i.e. it eliminates uncertainties arising out of superposition.

In Table 1 solutions of equations (15) and (28) are shown for three girders. The dimensions used in the calculations correspond to those of the specimens. Torsional rigidities have been calculated with the two different definitions of equivalent rod length as mentioned before.

6. Structure Assumed Pin-jointed

The foregoing method involves a considerable amount of numerical work in the solution of equations (15) and (28). A largely simplified, but less accurate answer is given by treating the bracing as tension or compression members simply supported at both ends. End moments and transverse forces become zero and F_b acts alone, viz.

$$M_b = M_{bt} = F_{bt} = 0$$

Note that the ball-jointed structure in this case represents a similar problem as dealt with by Batho (loc. cit.), however, the structure is still statically indeterminate and requires the Least Strain Energy method.

With equations (9) (13) and (14) the statically indeterminate quantities M_{yo} and F_b are obtained from

$$\left.\begin{aligned} \frac{\partial U}{\partial M_{yo}} &= 0 \\ \frac{\partial U}{\partial F_b} &= 0 \end{aligned}\right\} \quad . \quad . \quad . \quad . \quad . \quad (29)$$

It may be shown that M_{yo} is zero again.

Similarly to the infinite girder, the finite case is solved by the partial derivatives of U with respect to the unknown quantities

$$\left.\begin{aligned} \frac{\partial U}{\partial F_b} &= 0 \\ \frac{\partial U}{\partial M_{zo}} &= 0 \\ \frac{\partial U}{\partial F_{zo}} &= 0 \end{aligned}\right\} \quad . \quad . \quad . \quad . \quad . \quad (30)$$

where U is given by equations (25) (14) and (27).

Values of torsional rigidity by this method are shown in Table 1 for three girders.

TABLE 1.

Theoretical values of statically indeterminate quantities and torsional rigidity for girders A6, B6 and A1.

Girder	A6				B6				A1	
Type of solution	Structure rigid		Structure	Pin jointed	Structure rigid		Structure	Pin jointed	Rigid	Pin jointed
Equation	(15)	(28)	(29)	(30)	(15)	(28)	(29)	(30)	(28)	(30)
F_b/T	0·15511	0·15129	0·15689	0·15450	0·14779	0·14452	0·14916	0·14623	0·15456	0·15649
F_{bt}/T	0·00017	0·00019			0·00002	0·00004			0·00020	
M_b/T	—0·00109	—0·00129			—0·00038	—0·00094			—0·00135	
M_{bt}/T	0·00307	0·00333			0·00275	0·00307			0·00355	
M_{zo}/T		0·00073		0·00076		0·00081		—0·00016	0·00071	0·00080
F_{zo}/T		0·02661		0·02625		0·02347		0·02837	0·02663	0·02651
C_1/E		3·992 3·763		4·029 3·786		4·848 4·650		4·796 4·598	3·798 3·573	3·840 3·611
C_{oo}/E	4·403 4·103		4·352 4·054		5·402 5·139		5·347 5·085			
With eq. (3) C_b/E	4·329 4·042		4·294 4·007		5·308 5·057		5·247 4·997			
Experimental C/E	4·060				4·660				3·500	

Note : Upper figures for C are calculated using definition (*i*), lower figures using definition (*ii*) of equivalent length of rod (see section 2. 1.).

7. Non-Linear Characteristics

The experimental curves for torsional rigidity which were obtained from each girder show clearly that C does not remain constant even in the range where all internal stresses are below the yield point. This is due to the non-linear behaviour of the bracing rods subjected to simultaneous axial compression and bending. These are the rods under compression and bending due to F_b and M_{bz} and M_{bt}, respectively. For practical purposes, the effect of M_{bz} may be neglected since $M_{bz} < M_{bt}$ and M_{bz} acts to produce double curvature whereas M_{bt} causes single curvature.

The bending moment at any point x from the end of the rod may be expressed by an approximate method[6] frequently used in the solution of problems involving combined axial and lateral loads. Thus the bending moment is

$$M = M_{bt}\left[1 + \frac{F_b(lx - x^2)}{2EI(1 - \alpha)}\right] \quad . \quad . \quad (31)$$

where $\alpha = \dfrac{F_b l^2}{\pi^2 EI}$ and l is the length of the rod between pin-ends. For the purpose of evaluating M, the length is not equal to our previous l_b. It will be assumed that the ends of the rods acting as columns are located at the mid-width of the channel flanges for the infinite girders and for the single-bay girders l terminates at the edges of the channel flanges since in the latter case flexure of the flange is prevented by the end plates.

The bending moment is no longer proportional to the applied torque and consequently the strain energy $\left(\text{can not be expressed in the form } \dfrac{UE}{T^2}\right)$ is not proportional to T^2.

Instead of U we may write $(U' + U_c)$ where U' is now the total strain energy due all forces and moments with the exception of M, having the form kT^2 where k is a constant, and U_c is the variable strain energy due to the non linear M. The latter can also be reduced as $\dfrac{U_c}{T^2}$ for any value of T.

The modified expression for torsional rigidity is given by

$$\frac{C}{E} = \frac{LT^2}{4(U' + U_c)E} \quad . \quad . \quad . \quad . \quad (32)$$

This can be expanded as a power series in T or calculated for individual values of T, the latter being preferable because of slow convergence of the series at large values of T.

Substituting equation (32) into (3), and remembering that only half the rods are under compression, equation (3) becomes

$$\frac{C}{E} = \frac{(n+1)LT^2}{4E[n(U\infty - \frac{1}{2}U\infty_{Mbt} + \frac{1}{2}U_c\infty) + (U_1 - \frac{1}{2}U_{1Mbt} + \frac{1}{2}U_{c1})]} \quad . \quad . \quad . \quad . \quad (33)$$

where U_{1Mbt} and $U\infty_{Mbt}$ are the strain energies due to M_{bt} for the finite and infinite case, respectively.

C—curves, based on equation (33) have been drawn in Appendix 1.

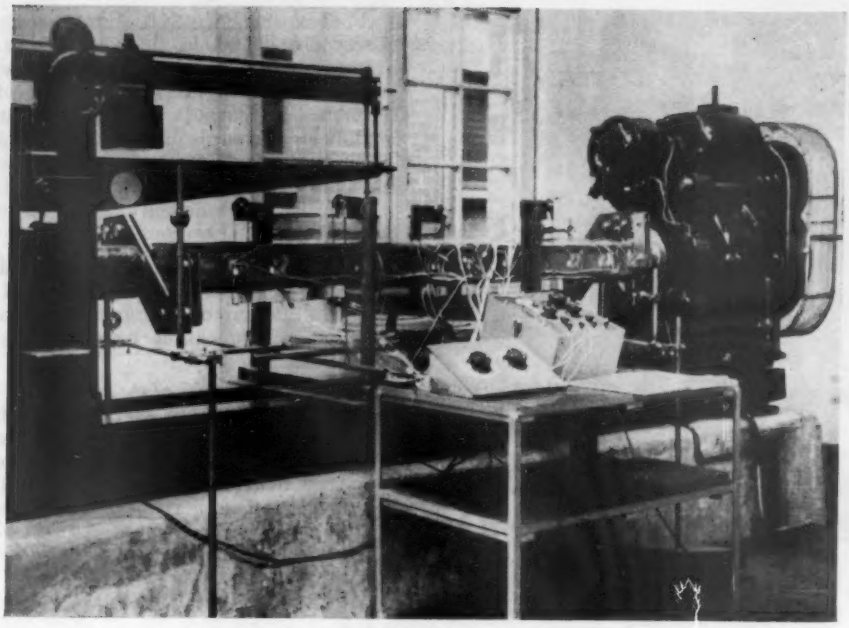

Fig. 9.

8. Experimental Investigation

Tests on full size girders were carried out to study the torsional properties and stress distribution in box section girders discussed in the Paper. The dimensions of each girder are shown in Appendix 2.

The size and length of the girders were limited by the load capacity and length of lead of the torsion machine, respectively. As the maximum length of the specimen that could be accommodated was six feet, two nominal lengths of six and one foot were chosen. Fig. 9 shows a 6 ft. girder fitted into the machine and ready for testing. A pure torque is applied to the specimen through a pair of link mechanisms provided with spherical roller bearings at all link joints. In this way it was possible to apply a pure torque irrespective of the deformations of the girder.

Curves of torsional rigidity plotted against applied torque are shown in Appendix 1.

Stresses were measured by strain gauges attached to various parts of the girder as shown on Figs. 10 and 11. Points of interest were mainly bracing rods under compression and, to a lesser extent, rods under tension. Stresses in the channel section were measured at $x = 0$ and $x = L/2$.

Internal forces and moments were calculated from strain readings corresponding to an increment of the applied torque of 40,000 in.-lb.

A complete set of forces and moments expressed in terms of T is shown in Table 2.

The non-linear changes of the internal forces and moments when measured against increasing applied torque is demonstrated in Figs. 12 and 13 showing values of F_b/T and M_{bt}/T for tensioned and compressed rods.

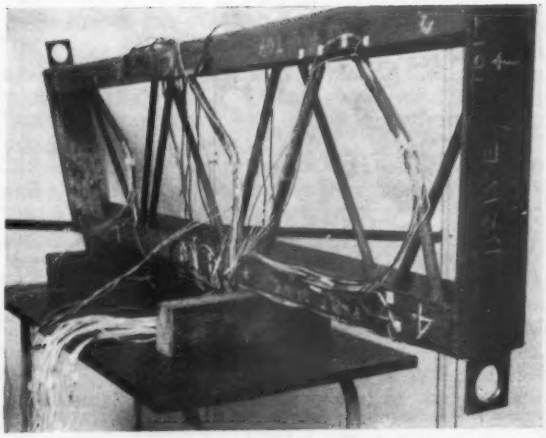

Fig. 10.

8.1 *Mode of Failure of Girders*

Girders A6 (6 foot) and 1A (1 foot) were tested to failure whereas girder B6 (6 foot) was loaded only within the elastic range.

(a) *Test on Girder A6*—Failure of the girder was initiated by simultaneous buckling and yielding of rods under compression. The first rod to buckle was one connected to the centre of the girder and yielding commenced at 75,400 in.-lb.

After some further twisting, a compression rod midway between centre and end of the girder buckled, followed immediately afterwards by a rod reaching the end of the girder. The ultimate load recorded was 79,100 in.-lb. The deformed girder after a twist of approximately 18° is shown in Fig. 10.

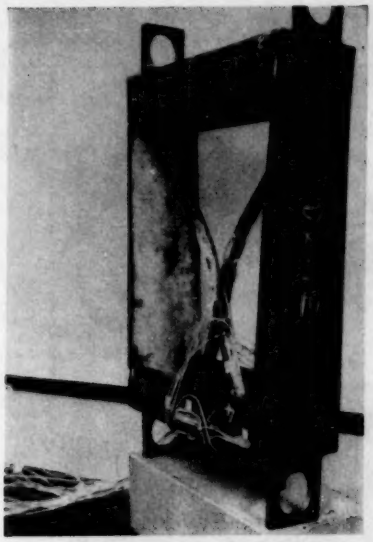

Fig. 11.

(b) *Test on Girder A1*—First signs of yielding were observed at 85,000 in.-lb. The yield was due to direct overstraining and no signs of flexure or buckling could be seen. A considerable amount of plastic strain developed at a steady rate at approximately constant load before inwards buckling of the bar took place. The ultimate load reached was 95,100 in.-lb.

The specimen after the test is shown in Fig. 11.

8.2 *Experiment Versus Analysis*

An examination of Table 2 shows that a considerable variation exists in the magnitudes of the forces and moments measured on different rods and parts of the channels. Two causes have been considered to be responsible.

(i) *Lack of uniformity of the girder itself*—All dimensions in Appendix 2 are averages. In fact, appreciable deviations were observed in the angle ψ and dimension b which is most important as far as stress distribution is concerned. Initial curvature of the rod, either inwards or outwards, will tend to increase or decrease respectively, the bending moment in the rod under compression.

TABLE 2.

Experimental values calculated from Strain Gauge readings.

GIRDER A6	F_b	F_{bt}	F_{zo}	M_b	M_{bt}	M_x	F_x	M_z	$(M_y)_{x=L/2}$
Rod Ia	$0{\cdot}1332T$* $0{\cdot}1428T$	$0{\cdot}00057T$		$-0{\cdot}00141T$	$0{\cdot}00928T$				
IIIa	$0{\cdot}1388T$* $0{\cdot}1441T$	$0{\cdot}00046T$		$-0{\cdot}00058T$	$0{\cdot}0148T$				
Va	$0{\cdot}1369T$			$-0{\cdot}00058T$	$0{\cdot}0122T$				
IIIb	$0{\cdot}1300T$			$-0{\cdot}00575T$	$0{\cdot}0128T$				
IIa	$0{\cdot}1269T$* $0{\cdot}1438T$	$0{\cdot}00066T$		$-0{\cdot}00406T$	$0{\cdot}0060T$				
Channel section 1—1			$0{\cdot}0115T$			$0{\cdot}00567T$	$0{\cdot}0774T$†	$0{\cdot}101T$†	$0{\cdot}013T$
3—3			$0{\cdot}0042T$			$0{\cdot}00917T$	$0{\cdot}100T$†	$0{\cdot}037T$†	$0{\cdot}005T$
4—4							0	0	$(0)x = o$
GIRDER A1									
Rod Ia	$0{\cdot}1253T$* $0{\cdot}1392T$	$0{\cdot}00068T$		$-0{\cdot}00407T$	$0{\cdot}0108T$				
Ib	$0{\cdot}1233T$* $0{\cdot}1590T$	$0{\cdot}00069T$		$-0{\cdot}00645T$	$0{\cdot}00995T$				
Channel section 1—1							$0{\cdot}0728T$†	$0{\cdot}099T$†	$0{\cdot}0075T$
GIRDER B6									
Rod Ia	$0{\cdot}127T$	$0{\cdot}00022T$		$-0{\cdot}0062T$	$0{\cdot}0132T$				
IIIa	$0{\cdot}126T$	$0{\cdot}00038T$		$-0{\cdot}0057T$	$0{\cdot}0176T$				
IIIb	$0{\cdot}127T$	$0{\cdot}00030T$		$-0{\cdot}0060T$	$0{\cdot}0178T$				
IVa	$0{\cdot}129T$				$0{\cdot}0121T$				
Channel section 3—3							$0{\cdot}118T$ — flange gauges $0{\cdot}141T$ — web ,,		
4—4							$0{\cdot}082T$ — web ,,		

Note. * refers to strain gauge readings at the ends of the rods, unmarked values are from gauges at midlength.
† these values may be $\pm$ depending on whether F_b is tensile or compressive.
All values correspond to $T_1 = 5000$, $T_2 = 45000$, $\Delta T = 40000$ in. lb.

(ii) *Localized and non-uniformly distributed stresses*—In calculating the internal forces and moments the assumption was made that all forces and moments were acting through centres of gravity and about neutral axes, respectively. This is not valid in this case. All forces and moments applied by the rod to the channel act through the weld at the inner surface of the flanges; thus axial direct stresses will not be uniformly distributed and this is demonstrated by the values of F_b and F_x for girders A6 and B6 in Table 2 ($F_x = -F_b cos\psi - F_{bt} sin\psi$).

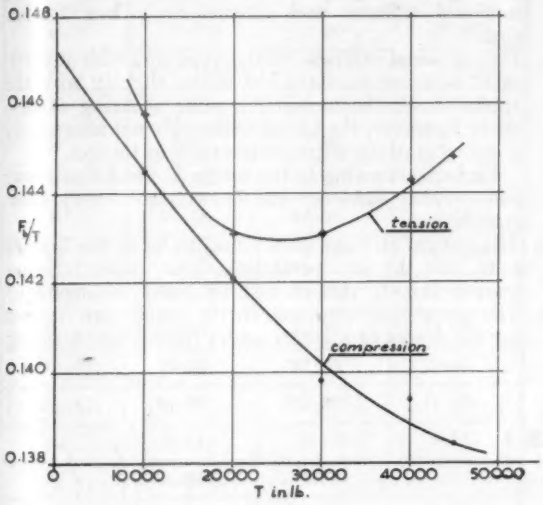

Fig. 12.

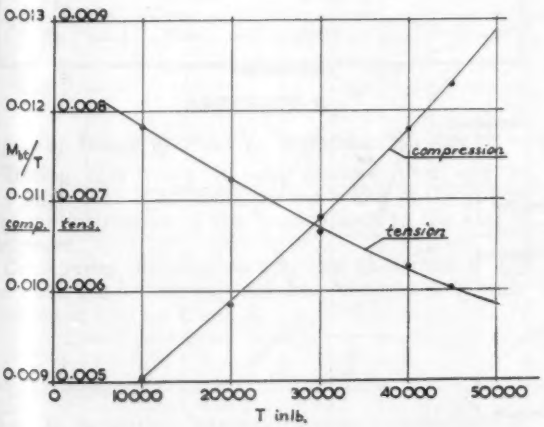

Fig. 13.

The deviation from simple beam theory type bending stress due to moments applied by the rods to the channel is possibly of a similar, if not larger magnitude. The presence of high local bending stresses was established beyond doubt by additional strain measurements.

In conclusion it may be said that the measured values in Table 2 which refer to the channel cannot therefore be compared with the analytical results. However, a comparison is more satisfactory for the bracing rods.

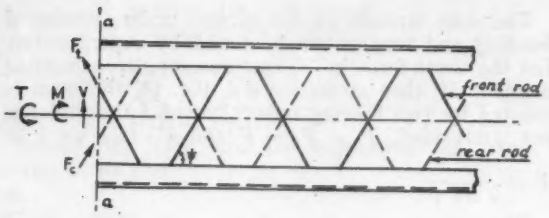

Fig. 14.

8.3 *Non-Linear Torsional Rigidity*

The graph showing C/E versus T in Appendix 1 indicates a gradual decrease in torsional rigidity until yielding or buckling load is reached at which stage the collapse of the girder is marked by a sharp increase in slope.

The assumption of constant ratios versus torque T of the internal forces and moments (with the exception of M_{bt}) is confirmed by Fig. 12 which shows a variation in F_b/T of only 6 per cent over the range of T.

The considerable variation in M_{bt}/T on the other hand, is seen in Fig. 13 where mean values of M_{bt}/T are plotted for compression and tension rod.

An interesting feature here is the fact that a larger rigidity $(C)_T = 0$ does not necessarily imply that the reduction in C with increasing T will be at a smaller rate, nor does a greater initial rigidity mean that a higher 'ultimate load' will be reached before buckling took place.

9. Application of Analysis to Design of Girders

A girder such as considered in this Paper, rarely is subjected to torsional load alone. As a structural member, the normal loading conditions are most likely to be such as to cause a bending moment and possibly axial compression.

From simple beam theory the bending moment and shear force capacities are given appropriately by

$$M = \sigma_w A_c D$$
$$V = (F_t + F_c)\ sin\ \psi$$

where σ_w = working stress in the compression member
D = distance between centres of gravity of channels
F_t, F_c = maximum permissible forces in the tension and compression rods, respectively.

The length of the bay is controlled on the one hand by bending requirements. For least weight, the bay may be made of such a maximum length for which the compression 'flange' is at the limit of elastic stability. This length and D will define the shear capacity of the girder for any rod size. The sections treated in this Paper have $\psi \doteqdot 60°$ which corresponds to a design for bending moment and at the same time maximum torsional rigidity (see Appendix 3).

When shear strength is of primary importance, maximum rod efficiency will be attained when the rods are sloping at 45°.

9.1 *Eccentric Load*

A twisting moment will be set up when the line of action of a transverse load does not pass through the centre of gravity of the section. Twisting of the section will take place until equilibrium is reached. The torque is now the sum due to initial eccentricity and eccentricity caused by twisting of the girder. The twist is calculated using the C value corresponding to equilibrium torque.

The true stresses in the girder under combined bending and torsion can be found by superposition. Let the shear force be V, corresponding to a bending moment M, then at section *a-a*, Fig. 14, the shear is resisted by two bracing rods. Provided the girder is not overloaded, $F_t = F_c = F$ and $V = 2F \sin \psi$ or $F = \dfrac{V}{2 \sin \psi}$.

The force in the channel at *a-a* is M/D causing tensile or compressive stress.

If a torque T is superimposed as shown at *a-a*, a compressive force $\alpha T = F'$ is introduced in both rods, and the resultant force in the rear rod is $(F_c + F')$ and for the front rod $(F_t - F')$. In the next bay the rear rod is under tension of $(F_t + F')$. Thus a non-symmetrical stress distribution is set up in the bracing with maximum and minimum values in the rear plane of rods.

Collapse of the girder will initiate in the rod under compression of $(F_c + F')$ or, substituting from above $\left(\dfrac{V}{2 \sin \psi} + \alpha T\right)$ where α is the constant obtained from the analysis of the girder subjected to torsion.

In the particular case of large bending moment and torque, the combined stresses in the channel ought to be checked as well as in the rods. The axial force in the channel due to T changes sign at each panel point and may be additive or subtractive to the uniform force caused by bending.

When checking the strength of a girder, the forces and moments obtained for the infinite length girder should be used. The difference between $(F_b)\infty$ and (F_b), was found to be small, nevertheless $(F_b)\infty$ is slightly larger thus representing the critical case.

This feature was confirmed experimentally by the mode of failure of girder A6 where rods under compression and furthest from the ends buckled first.

10. Conclusions

1. It has been shown that strain energy methods can usefully be employed in the calculation of the torsional stiffness and stresses in a box section girder.
2. The torsional stiffness of the type of girder investigated is is not constant but varies slightly with the applied load, the maximum value occuring at zero load. However, the initial stiffness is not necessarily a criterion of its ultimate strength in torsion.

   End effects owing to the method of end finish may considerably influence the behaviour of very short girders.
3. The critical stresses were found to be in the bracing rods, and the structural behaviour under torsional load is largely determined by their arrangement.
4. The method, as outlined, in the paper, can be used for the design of a girder under torsion and bending.

APPENDIX 1

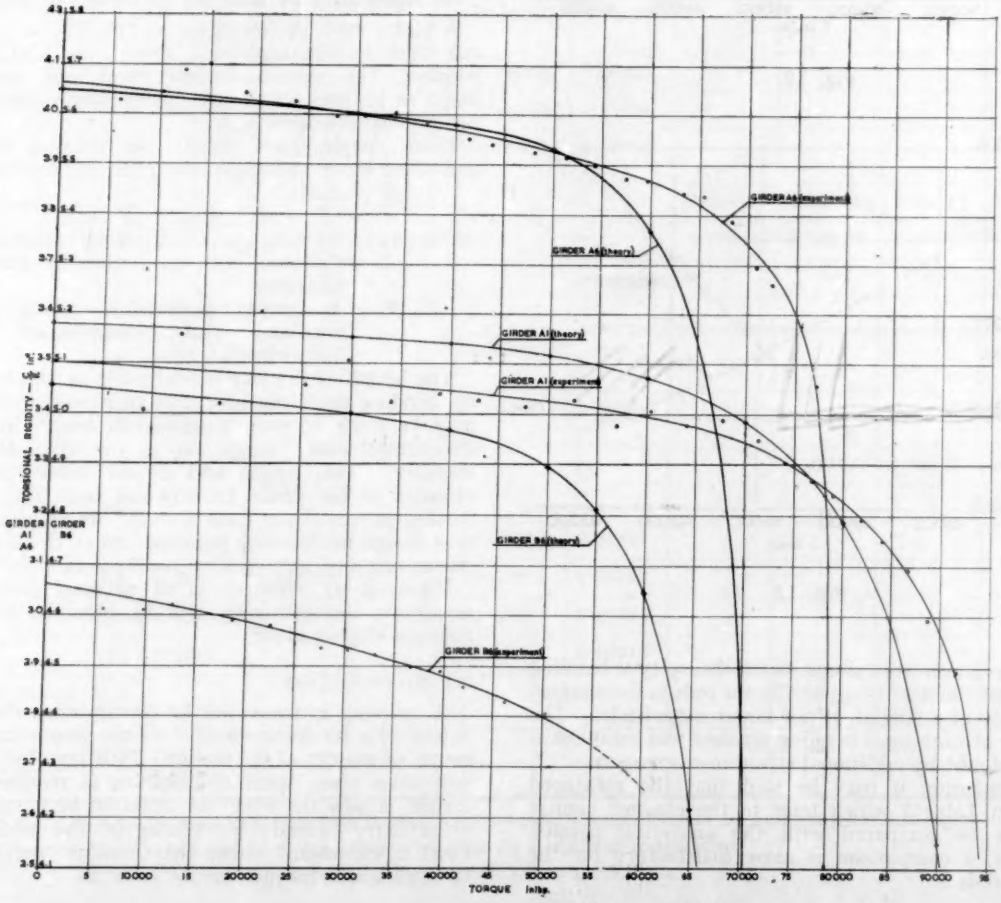

APPENDIX 2

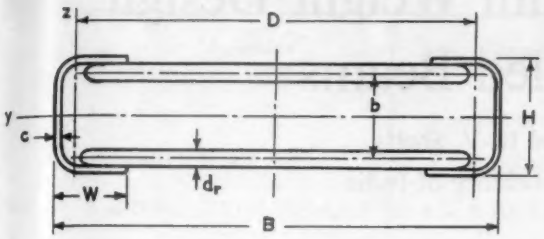

	A6	A1	B6
c	0·200	0·200	0·200
a	10·114	10·114	10·114
H	5·070	5·070	5·065
W	2·98	2·98	2·95
b	3·900	3·800	3·978
B	19·98	19·98	19·95
d_r	0·750	0·750	0·750
D	18·130	18·130	18·140
L	12·00	12·00	12·00
l_b (i)	22·00	22·00	20·20
l_b (ii)	23·82	23·82	21·35
I_y	8·111	8·111	8·117
I_z	1·815	1·815	1·777
ψ	59·75°	59·75°	55·79°
e	1·224	1·274	—0·224
c_p	0·375	0·375	0·375
b_p	5·00	5·00	5·00

APPENDIX 3

Effect of Length of Pitch on Torsional Rigidity

During this work it was realized that one of the major factors affecting the behaviour of the girders was the inclination of the bracing rods to the axis of the girder.

Considering the solution as given in Section 6, the rod force F_b can be expressed in terms of ψ by substituting in (29) for L and l_b

$$L = D_1 \cot \psi$$

and $$l_b = \frac{D_1}{\sin \psi}$$

where D_1 = vertical distance between intersections of centre lines of bracing rods.

Hence, after simplifying,

$$F_b = \frac{T b_1 \sin \psi \cos \psi}{a_1 \cos^3\psi + a_2 \cos\psi \sin^2\psi + a_3} \quad \cdots (35)$$

where $$b_1 = \frac{3(D + D_1)b(1+\mu)}{2ac^3}$$

$$a_1 = D_1\left[\frac{1}{A_c} + \frac{b^2}{12I_y} + \frac{e^2}{I_z}\right]$$

$$a_2 = \frac{3\left(2D + D_1 + \frac{D^2}{D_1}\right)b^2(1+\mu)}{2ac^3}$$

$$+ \frac{12(1+\mu)b^2}{5HcD_1} + \frac{(1+\mu)H}{2cD_1}$$

$$a_3 = \frac{D_1}{A_r}$$

and $e = \frac{1}{2}(D_1 - D)$.

Substituting (35) into the expression for strain energy U, we find

$$\frac{C\infty}{E} = \frac{D_1}{2}\left[\frac{a_1\cos^3\psi + a_2\cos\psi\sin^2\psi + a_3}{2c_1(a_1\cos^3\psi + a_2\cos\psi\sin^2\psi + a_3) - b_1^2\cos\psi\sin^2\psi}\right] \quad \cdots (36)$$

where $$c_1 = \frac{3(1+\mu)D_1}{4ac^3}$$

Curves of $C\infty/E$ and F_b/T calculated for girder A6 are shown in Fig. 15. It is interesting to note that the values of $C\infty$ is greatly dependent on ψ in the range used in engineering, reached a maximum at approximately 59°.

Force F_b, on the other hand, remains fairly constant at large values of ψ but increases rapidly when ψ falls below 45°. It may be seen that maximum stress in the bracing of the girder is reduced considerably by choosing a large value of ψ.

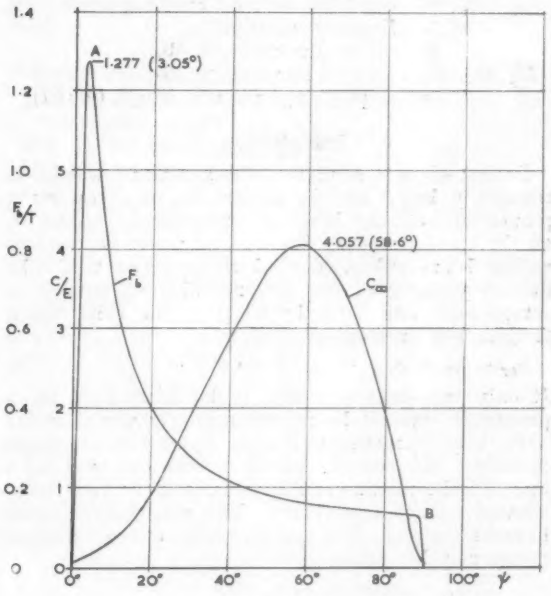

Fig. 15.

ACKNOWLEDGEMENTS

The work described in this paper was carried out in the Civil Engineering Department of the University of Melbourne, and the authors would like to thank Professor A. J. Francis for making facilities available.

The authors are indebted to Standard Steel Pty. Ltd., Melbourne, Australia for the girders tested.

References

1. Batho, C., *Engineering*, Oct. 15, 1915.
2. Pippard, A. J. S., and Douglas, W. D., *R. & M.* 736, Jan. 1921, *A.C.A.*, *v.*1, 1920/21.
3. Southwell, R. V., *R. & M.* No. 737, *A.C.A. v.*1, 1920/21.
4. Timoshenko, S., " Strength of Materials," 3rd Ed., *v.*1, p. 319.
5. Timoshenko, S. and Goodier, J. N., " Theory of Elasticity," 2nd Ed., p. 298.
6. Timoshenko, S., " Strength of Materials," 3rd Ed., v.2, p. 52.
7. Nolle, H., " On the torsional stiffness of box-section girders," Thesis presented *M.Eng. Sc.*, Melbourne, 1958.

A Method of Minimum Weight Design for Thin-Walled Beams

by S. Krishnan and K. V. Shetty
National Physical Laboratory of India

Notation

σ_{cr}	local buckling stress, p.s.i.
σ_b	bending stress, p.s.i.
σ_y	yield stress, p.s.i.
E	Young's modulus, p.s.i.
b	flange width parameter, in.
h	semi-web depth, in.
k	ratio h/b
t	wall thickness, in.
d	stiffener spacing, in.
n	number of stiffeners along each width.
a	area of material in stiffener section, in^2.
A	area of material in the beam section in^2.
I	moment of inertia, in^4.
K, K^1	constants for local buckling stress.
λ_1, λ_2	Lagrange multipliers.
M	external moment, in.-lb.
M_1, M_2, M_3	reduced moments, in.-lb.
θ	slope change per unit length (M/EI).

Introduction

Design of any structure for minimum weight is essentially based on the determination of optimum proportions on the basis of simultaneous failure in all the critical modes. The critical modes for a thin-walled beam subjected to bending loads would be due to yielding of the extreme fibre in tension or compression and local buckling of the compression flange. For simultaneous failure

$$\sigma_{cr} = \sigma_b = \sigma_y \quad . \quad . \quad . \quad . \quad . \quad . \quad (1)$$

If only two quantities are to be determined for a particular type of beam, equation (1) would suffice to fix fully optimum dimensions. Apart from the modes of failure referred to, special restrictions such as a limit on the maximum slope change may have to be allowed for in certain cases. This means there would be one more restriction and the conditions for optimum design may be expressed as

$$\sigma_{cr} = \sigma_b = \sigma_\theta = \sigma_y$$
$$\text{and} \quad \theta = \theta_y \quad . \quad . \quad . \quad . \quad . \quad . \quad (2)$$

where σ_θ represents the stress corresponding to the limiting slope change per unit length and θ_y the limiting slope change per unit length corresponding to the yield stress σ_y.

It would also be possible to use these equations to determine optimum proportions in terms of a structural loading coefficient[1] or a structural index[2]. However, a direct approach to the problem of designing for least weight may be made by minimising weight or area of material in the cross-section subject to the restraining conditions expressed by equations 1 and 2.

In this paper formulas have been derived for optimum dimensions of thin-walled I-, channel, and box sections with and without lips, and with and without stiffeners. Curves from which optimum dimensions may be directly read have also been plotted for steel and Al-alloy.

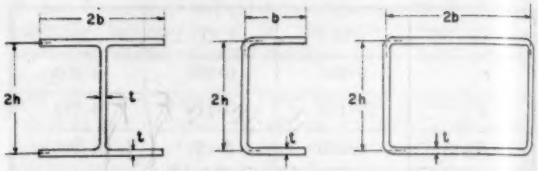

Fig. 1a.—Unstiffened Sections.

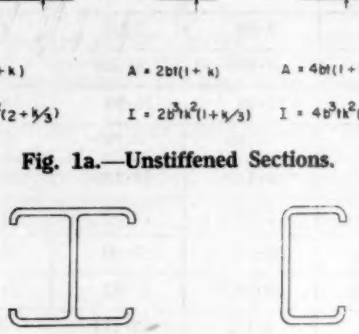

Fig. 1b.—Lipped Sections.

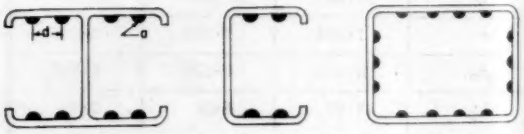

Fig. 2.—Stiffened Sections.

Theory

Unstiffened Sections :

Figs. 1a and 1b describe unstiffened I-, channel, and box sections with dimensions and sectional properties as shown. In deriving expressions for the optimum dimensions the following assumptions are made :—

1. The flange and the web are of the same thickness.
2. The web-depth is related to the flange-width by a ratio k which is treated as a variable.
3. The lips, in the case of lipped sections, change only the end condition of the outstanding flanges and do not appreciably contribute to the area and moment of inertia of the section.
4. The flange width b is determined by the known value of the yield stress thus having only one restraining condition and two variables t and k. Substituting corresponding terms for σ_{cr} and σ_b in equation 1, the restraining conditions for the three types of sections may be written as

TABLE 1

I-Section	*Channel Section*	*Box Section*
$k = 1{\cdot}3$	$k = 0{\cdot}646$	$k = 0{\cdot}646$
$t = 0{\cdot}541[M/KE]^{1/3}$	$t = 0{\cdot}86[M/KE]^{1/3}$	$t = 1{\cdot}084[M/K'E]^{1/3}$
$b = 0{\cdot}541(KE)^{1/6}M^{1/3}\sigma_y^{-1/2}$	$b = 0{\cdot}86(KE)^{1/6}M^{1/3}\sigma_y^{-1/2}$	$b = 0{\cdot}542(K'E)^{1/6}M^{1/3}\sigma_y^{-1/2}$

$$KE(t/b)^2 = \frac{M}{2t_b^2k(2 + k/3)} \quad \text{(I-Section)}$$

$$KE(t/b)^2 = \frac{M}{2t_b^2k(1 + k/3)} \quad \text{(Channel Section)}$$

$$K^1E(t/2b)^2 = \frac{M}{4t_b^2k(1 + k/3)} \quad \text{(Box Section)}$$

. . . . (3)

While minimising the area subject to the restraining conditions (3), Lagrange multiplier λ_1 is used leading to the variational equation

$$\delta(A + \lambda_1\varphi_1) = 0$$

Where A is the area of the material in the cross-section and φ_1 the restraining condition. The restraining condition φ_1 is expressed as

$$\varphi_1 = \sigma_{cr} - \sigma_b = 0$$

Differentiating with respect to t and k

$$\frac{\partial A}{\partial t} + \lambda_1 \frac{\partial \varphi_1}{\partial t} = 0$$

$$\frac{\partial A}{\partial k} + \lambda_1 \frac{\partial \varphi_1}{\partial k} = 0$$

. . . . (4)

Substituting for the derivatives of A and φ_1 in equations (4)

$$2b(2 + k) + \lambda_1 3t^2k(2 + k/3) = 0$$
$$2bt + \lambda_1 t^3(2 + 2k/3) = 0$$

. . (I-Section)

$$2b(1 + k) + \lambda_1 3t^2k(1 + k/3) = 0$$
$$2bt + \lambda_1 t^3(1 + 2k/3) = 0$$

. (Channel Section)

$$4b(1 + k) + \lambda_1 3t^2k(1 + k/3) = 0$$
$$4bt + \lambda_1 t^3(1 + 2k/3) = 0$$

. . (Box Section)

. . . . (5)

By eliminating λ_1 from each pair of equations solutions for t and k are obtained from the resulting equation together with the corresponding restraining condition. The results are shown in Table I.

Coefficient K for unlipped sections and K^1 for lipped and box sections are read from standard curves, and found to be 0·45 and 3·6 respectively[3]. Values of t and b have been computed for a range of moments 1,000 to 50,000 in.-lb. for unlipped steel and Al-alloy sections and plotted in Figs. 3 and 4. The compressive failure stress has been assumed to be 44,000 p.s.i. for Al-alloy and 40,000 p.s.i. for steel. Young's modulus E is taken as $10{\cdot}3 \times 10^6$ p.s.i. for Al-alloy and 30×10^6 p.s.i. for steel. For lipped I- and channel sections, the same solutions as for unlipped sections would apply except that K will have to be replaced by K^1.

Stiffened Sections :

Fig. 2 shows the stiffened I-, channel and box sections with dimensions and sectional properties marked. The assumptions used in this case are :—

1. The web and flange are of the same thickness.
2. The web-depth is related to the flange-width by a ratio k.
3. The web stiffeners do not contribute appreciably to the moment of inertia and they are ignored for this purpose.
4. There is a limit on the slope change which is reached when simultaneous failure occurs due to bending stress and local buckling.
5. The stiffeners are of equal area and uniformly spaced.

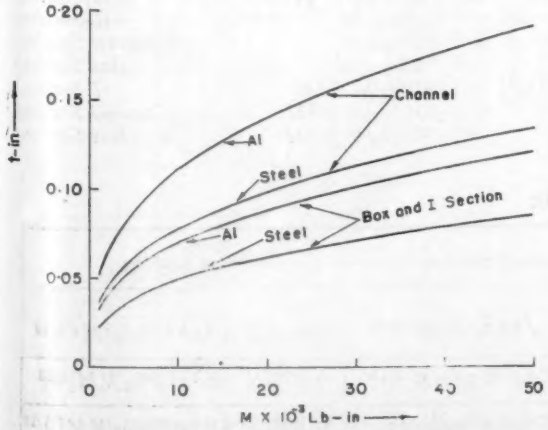

Fig. 3.—*t vs M* curves for unstiffened Al-Alloy and Steel Sections.

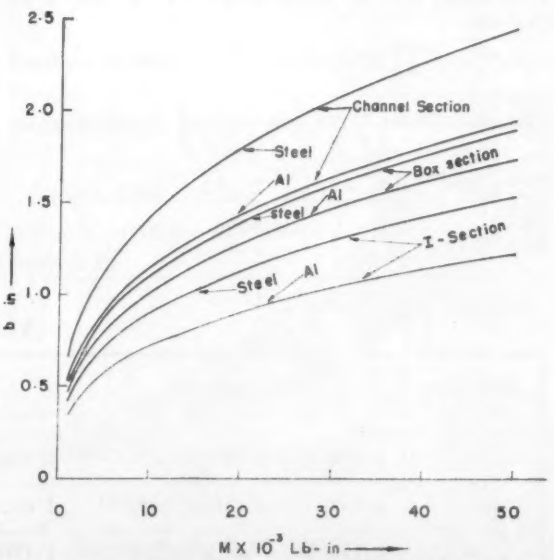

Fig. 4.—*b vs M* curves for unstiffened Al-alloy and steel sections.

Substituting the appropriate terms for σ_{cr} and σ_b in equation 2 and for a limiting value of slope change per unit length the restraining conditions for the three types of sections may be expressed as

$$K^1E(t/d)^2 = \frac{M}{2b^2k[t(2+k/3)+2a/d]}$$

$$\theta = \frac{M}{E \cdot 2b^3k^2[t(2+k/3)+2a/d]} \quad (I\text{-}Section)$$

$$K^1E(t/d)^2 = \frac{M}{2b^2k[t(1+k/3)+a/d]}$$

$$\theta = \frac{M}{E \cdot 2b^3k^2[t(1+k/3)+a/d]} \quad (Channel\ Section)$$

$$K^1E(t/d)^2 = \frac{M}{4b^2k[t(1+k/3)+a/d]}$$

$$\theta = \frac{M}{E \cdot 4b^3k^2[t(1+k/3)+a/d]} \quad (Box\ Section)$$

. . . . . (6)

With the aid of Lagrange multipliers λ_1 and λ_2 the area A is minimised subject to the restraining conditions (6) giving the variational equation

$$\delta(A + \lambda_1\varphi_1 + \lambda_2\varphi_2) = 0$$

Where φ_1 and φ_2 are the restraining conditions. The restraining conditions φ_1 and φ_2 are expressed as

$$\varphi_1 = \sigma_{cr} - \sigma_b = 0$$

$$\varphi_2 = \frac{M}{EI} - \theta = 0$$

Differentiating with respect to t, d, and b

$$\frac{\partial A}{\partial t} + \lambda_1\frac{\partial\varphi_1}{\partial t} + \lambda_2\frac{\partial\varphi_2}{\partial t} = 0$$

$$\frac{\partial A}{\partial d} + \lambda_1\frac{\partial\varphi_1}{\partial d} + \lambda_2\frac{\partial\varphi_2}{\partial d} = 0$$

$$\frac{\partial A}{\partial b} + \lambda_1\frac{\partial\varphi_1}{\partial b} + \lambda_2\frac{\partial\varphi_2}{\partial b} = 0$$

. . . . . (7)

Substituting for the derivatives of t, d, and b in equations 7.

$$2b(2+k)+\lambda_1\frac{b^2k}{d^2}\left[3t^2(2+k/3)+\frac{4at}{d}\right]+\lambda_2b^3k^2(2+k/3)=0$$

$$-4ab/d^2-\lambda_1t^2b^2k\left[\frac{2t}{d^3}(2+k/3)+6a/d^4\right]-\lambda_2b^2k^2\cdot 2a/d^2=0$$

$$2[t(2+k)+2a/d]+\lambda_1\frac{t^2k}{d^2}\cdot 2b\,[t(2+k/3)+2a/d]$$
$$+\lambda_2 3b^2k^2[t\,(2+k/3)+2a/d]=0 \quad (I\text{-}Section)$$

$$2b(1+k)+\lambda_1\cdot\frac{b^2k}{d^2}\left[3t^2(1+k/3)+\frac{2at}{d}\right]$$
$$+\lambda_2\cdot b^3k^2(1+k/3)=0$$

$$-2ab/d^2-\lambda_1\cdot t^2b^2k\left[\frac{2t}{d^3}(1+k/3)+3a/d^4\right]$$
$$-\lambda_2b^3k^2a/d^2=0$$

$$2[t(1+k)+a/d]+\lambda_1\cdot\frac{t^2k}{d^2}\cdot 2b[t(1+k/3)+a/d]$$
$$+\lambda_2\cdot 3b^2k^2\,[t(1+k/3)+a/d]=0 \quad (Channel\ Section)$$

$$4b(1+k)+\lambda_1\frac{b^2k}{d^2}\left[3t^2(1+k/3)+\frac{2at}{d}\right]$$
$$+\lambda_2b^3k^2(1+k/3)=0$$

$$-4b(1+k)\frac{a}{d^2}-\lambda_1\cdot t^2b^2k\left[\frac{2t}{d^3}(1+k/3)\right.$$
$$\left.+3a/d^4\right]-\lambda_2b^3k^2a/d^2=0$$

$$4(1+k)\,(t+a/d)+\lambda_1\cdot\frac{t^2k}{d^2}\cdot 2b[t(1+k/3)$$
$$+a/d]+\lambda_2\cdot 3b^2k^2[t(1+k/3)+a/d]=0$$
$$(Box\ Section)$$

. . . . . (8)

λ_1 and λ_2 are eliminated from each set of three equations, and the resulting equation together with the corresponding two restraining conditions yield solutions for b, t, and d. The flange width b divided by the stiffener spacing d gives the number of flange stiffeners n. The results are given in Table II.

The various functions f, g and h of k are as defined in the appendix. The results in Table II may be grouped together in the following form into one set of solutions which can be readily applied to any section :—

$$b = [K'E^{-4}a^{-2}\theta^{-5}M_1^4]^{1/13}$$
$$t = [K'^{-3}E^{-1}a^6\theta^2M_2]^{1/13}$$
$$n = [K'^{-2}E^{-5}a^{-9}\theta^{-3}M_3^5]^{1/13}$$

. . . . . (9)

Where

$$M_1 = 1{\cdot}506\,[f_1(k)]^{1/4}M \quad (I\text{-}Section)$$
$$= 1{\cdot}506\,[g_1(k)]^{1/4}M \quad (Channel\ Section)$$
$$= 0{\cdot}749\,[h_1(k)]^{1/4}M \quad (Box\ Section)$$
$$M_2 = 1{\cdot}507f_2(k)M \quad (I\text{-}Section)$$
$$= 1{\cdot}507g_2(k)M \quad (Channel\ Section)$$
$$= 0{\cdot}748h_2(k)M \quad (Box\ Section)$$
$$M_3 = 1{\cdot}504[f_3(k)\,]^{1/5}M \quad (I\text{-}Section)$$
$$= 1{\cdot}504\,[g_3(k)\,]^{1/5}M \quad (Channel\ Section)$$
$$= 0{\cdot}749\,[h_3(k)\,]^{1/5}M \quad (Box\ Section)$$

TABLE II

Particulars	*I-Section*	*Channel Section*	*Box Section*
b	$1{\cdot}134[K'E^{-4}a^{-2}\theta^{-5}f_1(k)M^4]^{1/13}$	$1{\cdot}134[K'E^{-4}a^{-2}\theta^{-5}g_1(k)M^4]^{1/13}$	$0{\cdot}915[K'E^{-4}a^{-2}\theta^{-5}h_1(k)M^4]^{1/13}$
t	$1{\cdot}032[K'^{-3}E^{-1}a^6\theta^2f_2(k)M]^{1/13}$	$1{\cdot}032[K'^{-3}E^{-1}a^6\theta^2g_2(k)M]^{1/13}$	$0{\cdot}978[K'^{-3}E^{-1}a^6\theta^2h_2(k)M]^{1/13}$
n	$1{\cdot}170[K'^{-2}E^{-5}a^{-9}\theta^{-3}f_3(k)M^5]^{1/13}$	$1{\cdot}170[K'^{-2}E^{-5}a^{-9}\theta^{-3}g_3(k)M^5]^{1/13}$	$0{\cdot}895[K'^{-2}E^{-5}a^{-9}\theta^{-3}h_3(k)M^5]^{1/13}$

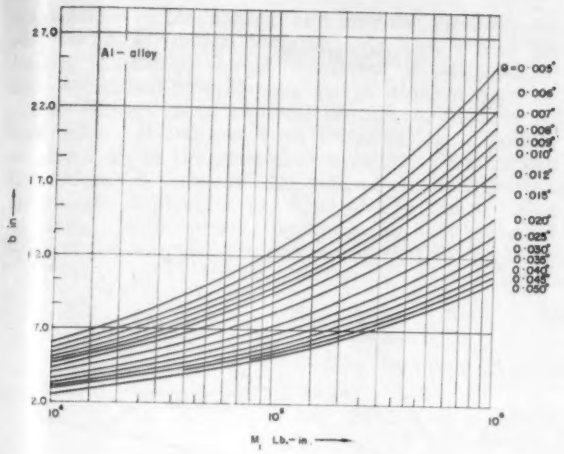

Fig. 5.—*b vs* M_1 curves for stiffened Al-alloy sections.

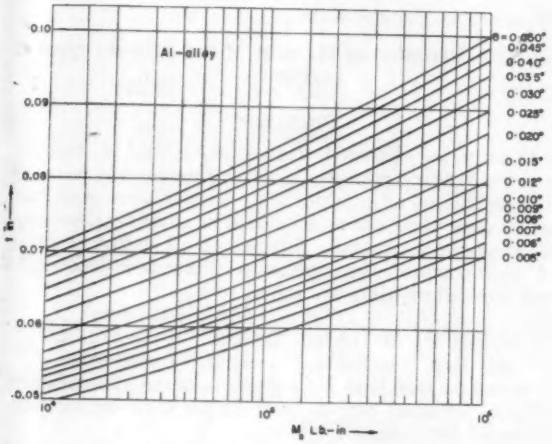

Fig. 6.—*t vs* M_2 curves for stiffened Al-alloy sections.

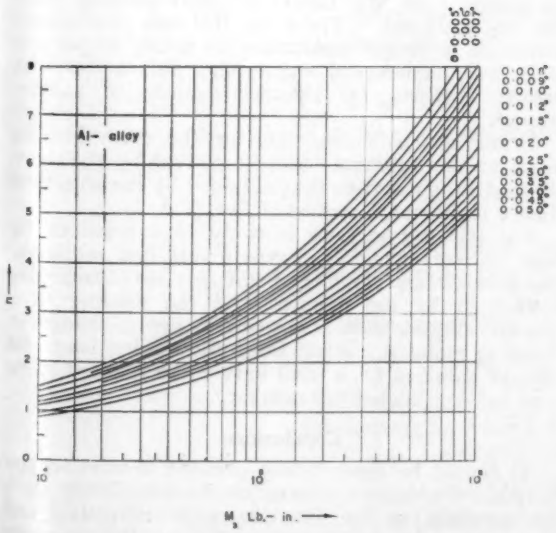

Fig. 7.—*n vs* M_3 curves for stiffened Al-alloy sections.

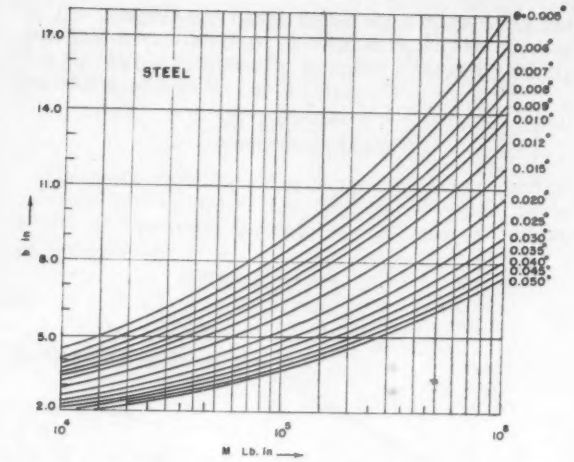

Fig. 8.—*b vs* M_1 curves for stiffened steel sections.

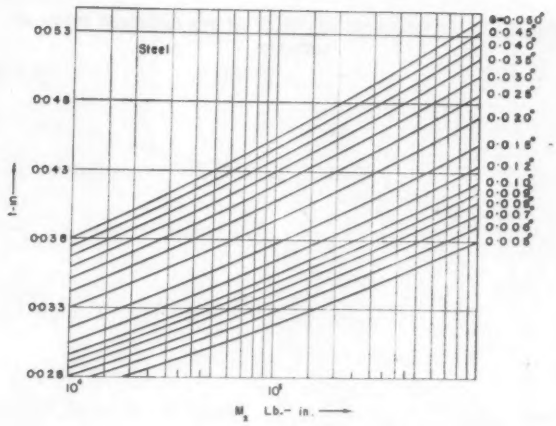

Fig. 9.—*t vs* M_2 curves for stiffened steel sections.

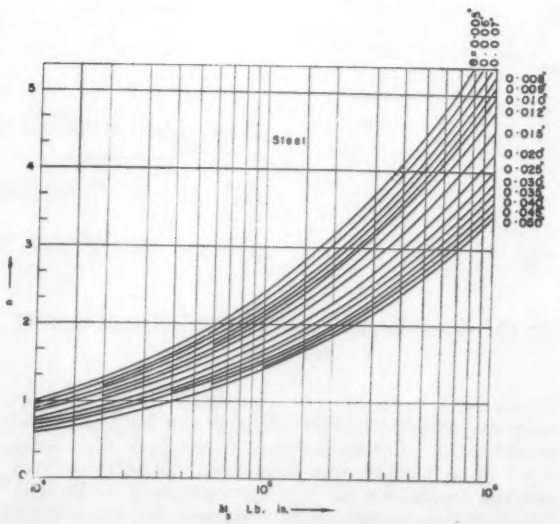

Fig. 10.—*n vs* M_3 curves for stiffened steel sections.

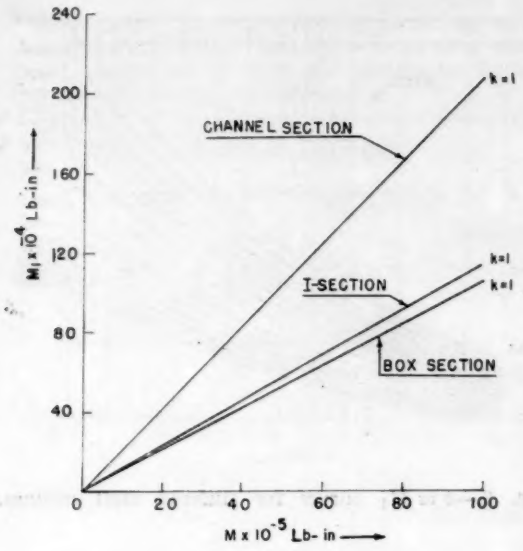

Fig. 11.—Variation of M_1 with M for different types of sections.

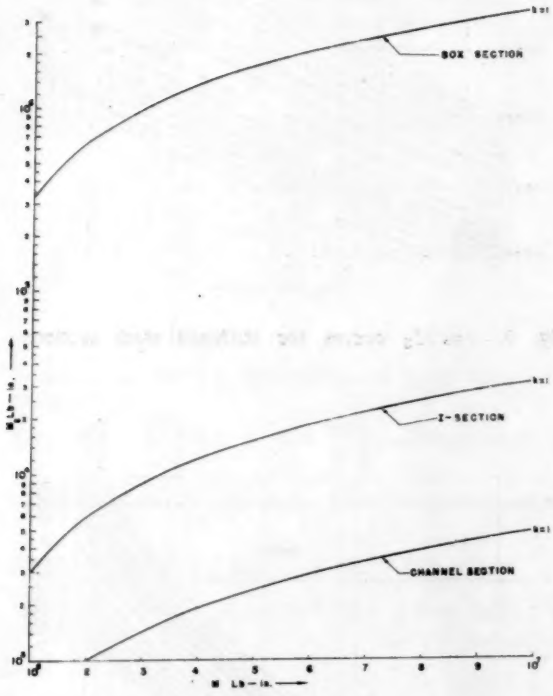

Fig. 12.—Variation of M_2 with M for different types of sections.

Values of b, t and n are computed for a range of moments 10,000 to 1,000,000 in.-lb. for both steel and Al-alloy and plotted in Figs. 5, 6, 7, 8, 9 and 10. A value of 0·2 in^2. has been used for stiffener area and the coefficient K' has been assumed to be 3·6. Corresponding values of M_1, M_2 and M_3 for a given M should be read from Figs. 11, 12 and 13 and used for reading b, t and n from the respective curves.

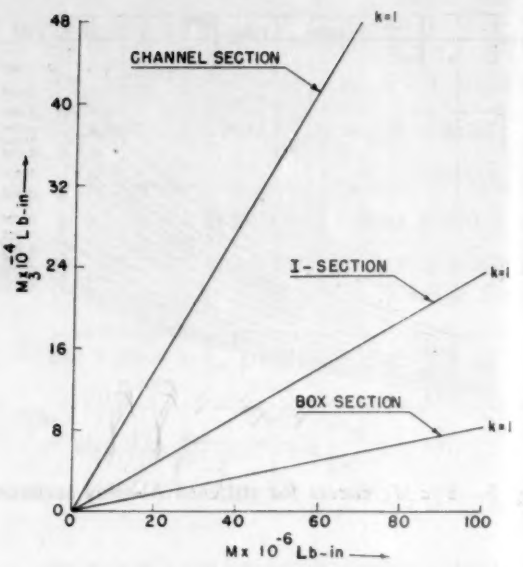

Fig. 13.—Variation of M_3 with M for different types of sections.

Discussion

It may be observed from Figs. 3 and 4 that for a given bending moment a larger thickness is required for unstiffened aluminium alloy section over steel but, at the same time, the width could be smaller. Choosing, for example, a channel subjected to a bending moment of 30,000 in.-lb. the optimum dimensions for steel and aluminium alloy are found to be

	t	b	*area*
Steel	0·110 in.	2·04 in.	0·742 sq/in.
Al-alloy	0·158 in.	1·62 in.	0·846 sq/in.

It can be seen that for a given moment the optimum Al-alloy channel can be over 50 per cent lighter than the steel counterpart.

Again from a comparison of the lipped and unlipped sections, it can be seen that K' being eight times K, optimum t for lipped channel is reduced to half that for unlipped while the value of b, for lipped channel is increased to $\sqrt{2}$ times the corresponding value for the unlipped. There is, therefore, an overall reduction in weight amounting to nearly 30 per cent if lipped channels are employed. This agrees with results obtained for channel sections in another paper[4].

It can also be shown that for the same bending moment the optimum I section derived by the above method is lighter than that obtained by the structural Index Technique described in Ref. (2) [5].

For stiffened sections a study of expressions (9) and the corresponding curves reveal that while the flange width and number of stiffeners are considerably influenced by the moment and the limiting slope change, the thickness is not so sensitive to changes in bending moment. While using the results, fractional figures obtained for n shall have to be rounded off to and the next higher full number.

Conclusions

It should be theoretically possible to solve for any number of unknown dimensions by introducing them as variables in the function to be minimised and imposing more restraining conditions. But too many restraining conditions may reduce the practical

applications of this method and may not yield reasonable results for design purposes. At least one of the leading parameters should be left out of minimisation and determined by other physical considerations.

One feature or advantage of this method is its generality. It has not been restricted to a definite value for σ_b in the general treatment. This enables the designer to have full freedom to choose his other parameters depending on what design stress value he takes. In the present paper the authors preferred to select the value for b in such a way that the buckling of the compression flange takes place only when the bending stress develops the value σ_y. The method can be readily extended to the plastic range by taking suitable functions for σ_{cr} and σ_b.

Acknowledgement

The work described in this paper is a part of the research programme of the National Physical Laboratory of India and is published with the permission of the Director.

Appendix

I-Section

The equations (8) for the I-Section may be rewritten as :—

$$\begin{aligned} &2d^2(2+k) + \lambda_1 bkt[3t(2+k/3) + 4a/d] \\ &\quad + \lambda_2 d^2b^2k^2(2+k/3) = 0 \\ &2ad + \lambda_1 bkt^2[t(2+k/3) + 3a/d] + \lambda_2 adb^2k^2 = 0 \\ &2d^2[t(2+k) + 2a/d] + \lambda_1 2bkt^2[t(2+k/3) + 2a/d] \\ &\quad + \lambda_2 \cdot 3d^2b^2k^2[t(2+k/3) + 2a/d] = 0 \end{aligned} \quad \cdots \quad (10)$$

Eliminating λ_1 and λ_2 from the above

$$\begin{vmatrix} bkt[3t(2+k/3)+4a/d] & d^2b^2k^2(2+k/3) & 2d^2(2+k) \\ bkt^2[t(2+k/3)+3a/d] & adb^2k^2 & 2ad \\ 2bkt^2[t(2+k/3)+2a/d] & 3d^2b^2k^2[t(2+k/3)+2a/d] & 2d^2[t(2+k)+2a/d] \end{vmatrix} = 0$$

Expanding

$$t^3d^3\left(16 + \frac{40k}{3} + \frac{28k^2}{9} + \frac{2k^3}{9}\right) + t^2d^2\left(16 + \frac{68k}{3} + \frac{10k^2}{3}\right)a - td\left(16 - \frac{28k}{3}\right)a^2 - 16a^3 = 0$$

Putting $td = ap$ the above equation may be expressed as :—

$$a_0p^3 + a_1p^2 - a_2p - a_3 = 0 \quad \cdots \quad (11)$$

Where

$$\begin{aligned} a_0 &= 72 + 60k + 14k^2 + k^3 \\ a_1 &= 72 + 102k + 15k^2 \\ a_2 &= 72 - 42k \\ a_3 &= 72 \end{aligned}$$

The two conditions (6) for the I-Section may be rewritten as :—

$$(t/d)^2b^2k[t(2+k/3) + 2a/d] = M/2K'E \quad \cdots \quad (12)$$

$$b^3k^2[t(2+k/3) + 2a/d] = M/2E\theta \quad \cdots \quad (13)$$

Dividing (12) by (13)

$$(t/d)^2 \cdot \frac{1}{bk} = \theta/K'$$

$$\therefore t = \left[\frac{a^2p^2\theta}{K'}bk\right]^{\frac{1}{4}}$$

Substituting for t and b in equation (13) gives

$$\begin{aligned} b &= 1{\cdot}134[K'E^{-4}a^{-2}\theta^{-5}k^{-13}\alpha^{-4}p^2M^4]^{1/13} \\ &= 1{\cdot}134[K'E^{-4}a^{-2}\theta^{-5}f_1(k)M^4]^{1/13} \\ &= [K'E^{-4}a^{-2}\theta^{-5}M_1^4]^{1/13} \end{aligned} \quad \cdots \quad (14)$$

Where

$$\alpha = p + 6p/k + 6/k$$
$$f_1(k) = k^{-13}\alpha_{-4}p^2$$
$$M_1 = 1{\cdot}134^{13/4}[f_1(k)]^{1/4}M$$

Similarly solving for t and d

$$t = 1{\cdot}032[K' - {}^3E - {}^1a^6\,\theta^2\alpha - {}^1p^7M]^{1/13}$$
$$= 1{\cdot}032[K' - {}^3E - {}^1a^6\,\theta^2 f_2(k)M]^{1/13}$$
$$= [K' - {}^3E - {}^1a^6\,\theta^2 M_2]^{1/13} \quad \ldots \quad (15)$$

Where

$$f_2(k) = \alpha^{-1}p^7$$
$$M_2 = 1{\cdot}032^{13}f_2(k)M$$

and

$$d = 0{\cdot}969[K'^3Ea^7\,\theta - {}^2\alpha p^6M - {}^1]^{1/13} \quad \ldots \quad (16)$$

Dividing b by d gives n.

Hence

$$n = 1{\cdot}170[K' - {}^2E - {}^5a - {}^9\theta - {}^3k - {}^{13}\alpha - {}^5p - {}^4M^5]^{1/13}$$
$$= 1{\cdot}170[K' - {}^2E - {}^5a - {}^9\theta - {}^3f_3(k)M^5]^{1/13}$$
$$= [K' - {}^2E - {}^5a - {}^9\theta - {}^3M_3{}^5]^{1/13} \quad \ldots \quad (17)$$

Where

$$f_3(k) = k^{-13}\alpha - {}^5p - {}^4$$
$$M_3 = 1{\cdot}170^{13/5}[f_3(k)]^{1/5}M$$

Channel Section

By a similar reasoning the equation corresponding to 11 in the case of channel section can be shown to be

$$a_0q^3 + a_1q^2 - a_2q - a_3 = 0 \quad \ldots \quad (18)$$

Where

$$a_0 = 18 + 30k + 14k^2 + 2k^3$$
$$a_1 = 18 + 51k + 15k^2$$
$$a_2 = 18 - 21k$$
$$a_3 = 18$$
$$q = td/a$$

and

$$b = 1{\cdot}134[K'E - {}^4a - {}^2\theta - {}^5k - {}^{13}\beta - {}^4q^2M^4]^{1/13}$$
$$= 1{\cdot}134[K'E - {}^4a - {}^2\theta - {}^5g_1(k)M^4]^{1/13}$$
$$= [K'E - {}^4a - {}^2\theta - {}^5M_1{}^4]^{1/13} \quad \ldots \quad (19)$$

$$t = 1{\cdot}032[K' - {}^3E - {}^1a^6\,\theta^2\beta - {}^1q^7M]^{1/13}$$
$$= 1{\cdot}032[K' - {}^3E - {}^1a^6\,\theta^2 g_2(k)M]^{1/13}$$
$$= [K' - E - {}^1a^6\,\theta^2 M_2]^{1/13} \quad \ldots \quad (20)$$

$$n = 1{\cdot}170[K'^{-2}E - {}^5a - {}^9\theta - {}^3k - {}^{13}\beta - {}^5q - {}^4M^5]^{1/13}$$
$$= 1{\cdot}170[K' - {}^2E - {}^5a - {}^9\theta - {}^3g_3(k)M^5]^{1/13}$$
$$= [K' - {}^2E - {}^5a - {}^9\theta - {}^3M_3{}^5]^{1/13} \quad \ldots \quad (21)$$

Where

$$\beta = q + 3q/k + 3/k$$
$$g_1(k) = k^{-13}\beta - {}^4q^2$$
$$M_1 = 1{\cdot}134^{13/4}[g_1(k)]^{1/4}M$$

$$g_2(k) = \beta - {}^1q^7$$
$$M_2 = 1{\cdot}032^{13}g_2(k)M$$
$$g_3(k) = k^{-13}\beta - {}^5q - {}^4$$
$$M_3 = 1{\cdot}170^{13/5}[g_3(k)]^{1/5}M$$

Box Section

The cubic equation in this case is

$$a_0r^3 + a_1r^2 - a_2r - a_3 = 0 \quad \ldots \quad (22)$$

Where

$$a_0 = 36 + 24k + 4k^2$$
$$a_1 = 36 - 15k - 9k^2$$
$$a_2 = 36 + 39k$$
$$a_3 = 36$$
$$r = td/a$$

and

$$b = 0{\cdot}915[K'E - {}^4a - {}^2\theta - {}^5k - {}^{13}\gamma - {}^4r^2M^4]^{1/13}$$
$$= 0{\cdot}915[K'E - {}^4a^{-2}\theta - {}^5h_1(k)M^4]^{1/13}$$
$$= [K'E - {}^4a^{-2}\theta - {}^5M_1{}^4]^{1/13} \quad \ldots \quad (23)$$

$$t = 0{\cdot}978[K' - {}^3E - {}^1a^6\,\theta^2\gamma - {}^1rqM]^{1/13}$$
$$= 0{\cdot}978[K' - {}^3E - {}^1a^6\,\theta^2 h_2(k)M]^{1/13}$$
$$= [K' - {}^3E - {}^1a^6\,\theta^2 M_2]^{1/13} \quad \ldots \quad (24)$$

$$n = 0{\cdot}895[K'^{-2}E - {}^5a - {}^9\theta - {}^3k - {}^{13}\gamma - {}^5r - {}^4M^5]^{1/13}$$
$$= 0{\cdot}895[K' - {}^2E - {}^5a - {}^9\theta - {}^3h_3(k)M^5]^{1/13}$$
$$= [K' - {}^2E - {}^5a - {}^9\theta - {}^3M_3{}^5]^{1/13} \quad \ldots \quad (25)$$

Where

$$\gamma = r + 3r/k + 3/k$$
$$h_1(k) = k^{-13}\gamma - {}^4r^2$$
$$M_1 = 0{\cdot}915^{13/4}[h_1(k)]^{1/4}M$$
$$h_2(k) = \gamma - {}^1r^7$$
$$M_2 = 0{\cdot}978^{13}h_2(k)M$$
$$h_3(k) = k^{-13}\gamma - {}^5r - {}^4$$
$$M_3 = 0{\cdot}895^{13/5}[h_3(k)]^{1/5}M$$

References

1. Cox, H. L. & Smith, H. E., "Structures of Minimum Weight, Aeronautical Research Committee" (*R. & M.*, 1923), 1943.
2. Shanley, F. R., "Weight Strength Analysis of Aircraft Structures," McGraw-Hill Book Co. Inc., 1952.
3. Timoshenko, S., "Theory of Elastic Stability," McGraw-Hill Book Co. Inc., 1936.
4. Krishnan, S. & Bhandari, D. R., "Influence of Local Buckling on Light Gauge Steel Structural Elements," Presented at the *Indian Standards Convention*, November, 1958.
5. Krishnan, S. & Shetty, K. V., "On the Optimum Design of an I-Section Beam," *Journal of the Aero/Space Sciences*, Vol. 26, September, 1959, pp. 599.

Discussion

The Council would be glad to consider the publication of correspondence in connection with the above paper. Communications on this subject intended for publication should be forwarded to reach the Institution by August 31st, 1961.

Book Review

Theory and Practice of Arc Welding, 2nd Edition, by R. J. Sacks. (New York & London : D. van Nostrand Co., Inc., 1960). 9½ in. × 6½ in., 478 + xii pp. 45s.

This is the second edition of a textbook first published in 1943, and is based on an original course of study in arc welding theory and practice in accordance with the current practices in industry in America and the recommendations of the American Welding Society.

The first section presents fundamental welding theory and includes chapters on industrial use of arc welding, equipment, mild steel electrodes, joints and welds, the nature of iron and steel, testing and inspection, flame cutting and safety precautions. Questions are given at the end of each chapter. The second section presents a comprehensive welding training course and deals with manipulative skills.

The text of the new edition has been revised to bring it in line with current practice, many new photographs and diagrams have been included and two new chapters have been added.

Institution Notices and Proceedings

ORDINARY GENERAL MEETING

An Ordinary General Meeting of the Institution of Structural Engineers was held at 11, Upper Belgrave Street, London, S.W.1, on Thursday, 23rd March, 1961, at 5.55 p.m. Lt.-Colonel G. W. Kirkland, M.B.E.(Mil.), M.I.Struct.E., M.I.C.E., in the Chair.

The following members were elected in accordance with the Bye-Laws. Will members kindly note that the elections, as tabulated below, should be referred to when consulting the Year Book for evidence of membership.

STUDENTS

BROWNE, Geoffrey, of Luton, Beds.
COCKBILL, David, of Salisbury, Southern Rhodesia.
FERNANDO, Kalutarage Stanley, of Colombo, Ceylon.
HYDE, Stephen Arthur, of London.
JOHNSON, Alan Edward, of Wilmslow, Cheshire.
MBAEZUE, Joseph Ikecukwu, of Zaria, Nigeria.
PARKS, Anthony, of Middlesbrough, Yorks.
SALIM, Mohammad, of District Sheikhupura, West Pakistan.
SRIVASTAVA, Upendra Nath, B.Sc., of Gorakhpur, Uttar Pradesh, India.
WALKER, David Whinray, of Morecambe, Lancs.
WEM, Peter, of Middlesbrough, Yorks.
WOOD, Jonathan Guy Martin, of Frensham, Surrey.

GRADUATES

ADAMS, James Edward, of Sutton, Surrey.
ARTHERN, Frederick, of Stockport, Cheshire.
BEVAN, David Milton, of Winterbourne, Bristol.
BROWN, Brian Arthur, of Winchester, Hants.
CHANDRACHOOD, Madhukar Abaji, B.E., of Poona, India.
COLES, Brian Stanley, B.Sc., of Horley, Surrey.
CROCKER, John, of Loughborough, Leics.
DESAI, Chandrakant Sankalchand, B.E., of Bombay, India.
DHAR, Chaman Lal, B.Sc., of Bombay, India.
FROGGATT, Michael Trevor, of Leamington Spa, Warwicks.
GRANBY, Alan Frederick, of Liverpool, Lancs.
GREEN, Michael Henry, of Kingsworthy, Nr. Winchester, Hants.
HENNEY, Graham, of West Wickham, Kent.
HORLER, David Brian, of Whitchurch, Cardiff.
IMEGWU, Eugene Odili, Ph.D., B.Sc., of Bristol.
JADAV, Manhar Kalidas, B.E., of London.
KONG FUNG KEW, M.Sc., of Leeds.
MARTIN, Thomas Allan, B.Sc., of London.
MITRA, Gopal Chandra, B.Tech.(Hons.), of Cologne, Western Germany.
NIE, Peter, of London.
O'CALLAGHAN, Michael John, B.E., of Newport, Mon.
RANCE, Ronald John, of Tring, Herts.
SHER KAR KIT, Joseph, of Holmcroft, Staffs.
SOLANKI, Chhaganlal Dewji, B.E., of London.
STEER, Peter John, B.Sc., of Hounslow, Middlesex.
THAN, Aung, B.Sc., of Rangoon, Burma.
THIRUMAL, Paramalingam, B.Sc., of Kopay, Ceylon.
TOLAT, Vipin Natwarlal, B.E., of London.
UDEAJA, Agbasielo Pius, of London.

ASSOCIATE-MEMBER

ROWE, Roy Ernest, M.A., A.M.I.C.E., of Slough, Bucks.

MEMBER

MCNULTY, Jim, of East Didsbury, Manchester, 20.

TRANSFERS

Students to Graduates

BASU, Utpal Kumar, B.Sc., of Greenford, Middlesex.
BISHOP, John Leighton, of Solihull, Warwickshire.
CLEATOR, Michael John, of Harrow, Middlesex.
FULLER, Norman, of Manchester.
GOODWIN, David Laurence, of Sutton, Surrey.
HAWKER, Brian Howard, of Cardiff, Glam.
HOOPER, Jeremy, of Ilkley, Yorks.

Graduates to Associate-Members

ASKEY, Reginald Charles, of London.

Associate-Members to Members

BRIMER, Alexander, of Lagos, Nigeria.
BULLOCK, Dennis Terence, B.Sc., A.M.I.C.E., of Sutton Coldfield, Warwicks.
BUNCE, John Wallace, of East Ewell, Surrey.
CURSITER, William Nisbet, B.Sc., A.M.I.C.E., of Lagos, Nigeria.
DAVIS, Frank, of Mombasa, Kenya.
FRAENKEL, Peter Maurice, B.Sc.(Eng.), of London.
HARVEY, John Alan, B.Sc., A.M.I.C.E., of Salisbury, Wilts.
HERRING, Bernard Carroll, of Lagos, Nigeria.
MCNAUGHTON, Finlay Malcolm, A.M.I.C.E., A.M.I.Mun.E., of Bolton, Lancs.
MORAN, Thomas Francis, of Liverpool.
PINKNEY, John Dennis, of Scunthorpe, Lincs.
VERYARD, Joseph Gordon, of Gabalfa, Cardiff.

RE-ADMISSION

Associate-Membership

GREGORIAN, Goriune Thaddeus, of Sidcup, Kent.

OBITUARY

The Council regret to announce the deaths of Charles Dimond Conway BRAINE (Member), and Leslie Guest HARRIS (Retired Associate-Member).

RESIGNATIONS

Notification was given that the Council had accepted with regret the resignations of Raymond Victor CHATE (Member), William MCKAY (Jnr.) (Associate-Member), Saghayroon EL ZEIN, William Thexton LAWTON, Bent Mehl LUDVIGSEN, Ebenezer Olufunso ODEDAIRO, Michael John PUNCH (Graduates), Thomas Neville WELLS (Student).

FORTHCOMING MEETINGS

The following meetings will be held at 11, Upper Belgrave Street, London, S.W.1.

Thursday, 25th May, 1961

Ordinary General Meeting for the election of members at 5.55 p.m., followed by the Annual General Meeting at 6 p.m.

Thursday, 22nd June, 1961

Ordinary General Meeting for the election of members 5 p.m.

INSTITUTION OF STRUCTURAL ENGINEERS BENEVOLENT FUND

The Annual General Meeting of the Voting Contributors to the Institution of Structural Engineers Benevolent Fund will be held at 11, Upper Belgrave Street, London, S.W.1, on Thursday, 25th May, 1961, at 6.20 p.m.

EXAMINATIONS, JANUARY, 1961

HOME AND OVERSEAS CENTRES

The Examinations of the Institution were held in January, 1961, at the usual centres in the United Kingdom, and overseas at the following centres :—

Accra, Aden, Aligarh, Auckland, Beirut, Bengazi, Bombay, Brazil, Cairns, Cairo, Calcutta, Cape Town, (South Africa), Christchurch (New Zealand), Colombo, Dar-Es-Salaam, Durban (South Africa), Harrisburg, Hong Kong, Johannesburg (South Africa), Kampala, Karachi, Khartoum, Kingston, Komati, Kuala Lumpur, Lagos, Lucknow, Lusaka, Madras, Mauritius, Melbourne, Montreal, Nairobi, Peru, Port Elizabeth (South Africa), Salisbury (Southern Rhodesia), Singapore, Sydney, Toronto, Trinidad, Vancouver, Wellington, (New Zealand) and Windhoek (South Africa).

One hundred and sixty-two candidates took the Graduateship Examination (103 at home and 59 overseas), and 808 candidates took the Associate-Membership Examination (650 at home and 158 overseas). Of these, 81 passed the Graduateship Examination (44 at home and 37 overseas) and 154 passed the Associate-Membership Examination (135 at home and 19 overseas).

The names of the successful candidates are :

Graduateship Examination

ADESOGA, Mobolaji
AFOLABI, Joseph Oduntan
ARTHUR, Roland Eric Brough
ATHALYE, Shridhar Mohaniraj
BHAT, Kaje Rama
CATO, Ross Edward
CHABLANI, Mohan Ghanshamdas
CHAN FOOK CHOY
CHIA CHER KENG
CHIU CHI SHING
DAS, Bishnu Pada
DAVE, Mrigendraray Mukundlal
DUKKER, Henri Frederic
EDWARDS, Elgin Winston
EMIABATA, Basiru Ademola
FARNWORTH, Frank
FEEROZ, Dawoodi Zainul
FERNANDEZ, Osborne Anthony
FORREST, Frank D.
GAJJAR, Chandrakant Damji
GLOVER, Benjamin Payne
GODFREY, Dan
GRAHAM, Ian
GRIFFITHS, John Charles
GUY, Kenneth
HAQUE, Malik Israrul
HINGORANI, Kishin Bhagchand
HUGHES, Peter James
HUNTER, William Emmanuel
ISANEDIGHI, Okon Uwe
LAI SHUI KWAN
LARNER, Raymond James
LEE CHEOK HOE
LOCKE, Joseph
LOREILHE, Vasco
MCCARTAN, Peter John
MAGUIRE, Robert John
MANIAR, Priyavadan Umedlal
MILLER, Roy James
MOORES, Arthur Keith
NARASINGA RAO, Prodduturi
NOTICE, Ezekiel Stephen
OBIOZO, Leo Emmanuel
OGUNSOLA, Thompson Olusola
OKAFOR, Ebenezer Chikwudozie
OLIVEIRA, Denis Ernest Ligorio
OMER, Awadalla Mohamed
ONUOHA, Nicholas Onyemauna
OWEN, John Alan
PAO WEI KANG
PARSONS, Eric Henry
PATEL, Kantilal Purushottamdar
PAUL, Iqbal Singh
PIERIS, Kurukulasuriya Justin Joseph S.
PITOT, Miss M. A. G.
POTGIETER, Theodorus Daniel
RAHA, Jogalrata
REID, Michael Irwin
RIZVI, Aulad Hussain
ROTHWELL, Conrad
SAFRI, T. L.
SALAKO, James Adebayo
SCHROEDER, Werner Otto Esmarch
SCHULER, Ronald Manfred
SESHAGIRI RAO, Kompella Venkatu S.
SHARMA, Har Bhagwan
SHASTRI, M. K.
SINGH, Dharam
SIVALINGAM, Gunaretnam
SMITH, Peter William
TANG HUNG CHUN
THOMAS, Warwick
TOWLER, Malcolm Philipson
VAMADEVAN, Nagalingam
WEBB, Ernest George
WESSIER, Bernard Eugene
WHELAN, Peter Denis
WONG CHING WAH
WRIGHT, Brian Allen
WROE, Herbert Brian
YUNG, Oliver Hon Bun

Associate-Membership Examination

ABU-SITTA, Salman Husein
ANDERSON, David Graham
AVIS, Peter Derek
BEAMAN, Jack
BENNETT, John David
BHOGAL, Harbans Singh
BISHOP, Colin Charles
BLASZYK, Tadeusz
BOYCE, Michael David
BRIGHT, Norman John
BROWN, Roy Charles
BULL, Geoffrey Michael
BUNN, David Michael
BURNETT, Walter
BUSH, Kenneth Donald
CARSON, Paul Frederick
CHANDA, Kanak Kumar
CHATARJEA, Sukhenda
CHOPRA, Narindar Nath
CLARKE, Francis Gerard
CLEMENTS, Alfred Cecil
CLOUGH, Norman
CORBETT, Brian Oliver
CORRY, John Percival
COX, Anthony James
COYNE, Terence
CROSS, John Henry
CRUDDAS, Edward Alan
DEAKIN, William Herbert
DIXON, Raymond James
DODD, Harry Thomas
DODD, James Michael
DOUET, Louis Maurice

DOUGLAS, James P. D.
DRAKE, Michael John
DUTT, Nihar Kusum
EALEY, Michael John
EDWARDS, William John Stephen
ELLISON, Morville Vernon
EVANS, David Geoffrey Rhys
FAIRWEATHER, Roy Leonard
FARSIDES, Costa Pavlou
FITZJOHN, Allan Arthur
FLANAGAN, George Edgar
FLEMING, Ian Doyle
FRASER, Frank Kojo
FRIBBANCE, William Lawrence
GACH, Jerzy
GHOSH, Srikumar
GILLIBRAND, William
GRAY, Bruce Alan
GREAVES, Brian Eric
GRIEVE, Neil Macpherson
GROVE, James Arthur
HADDOCK, Geoffrey
HAGENBACH, Paul
HALESTRAP, Terence Leonard
HALL, Conrad
HALLET, Rex
HARRIS, Clifford James
HARRIS, Martin Anthony
HARRIS, Peter William
HASTINGS, Joseph William
HERON, James Alexander Stewart
HOJEM, Peter Anthon
HOLROYD, Philip
HOLTUM, Ronald David
HOOKINS, Barrie Scott
HUFFORD, Howard Horace
HUGHES, John Allan
HUNT, David Charles Gowar
HUNTER, Ian Henderson
JAMES, Harold Cecil
JAY, Bernard Ensor
JEPSON, Wilfrid John
JORDAN, Edward John
KERNS, Donald Patrick
KING, Peter Henry
KULKARNI, H. M.
LAING, John Cranston
LAWRENCE, Hedley
LAWSON, Harland
LAXTON, David James
LI KUI WAI
LEIBNER, Rolf Otto
LIMNER, Thomas
LIPP, Lawrence
LOCKE, Joseph
LOUGHTON, Alan James
LOVELESS, Colin
LUDLAM, Donald Thomas
LUHAR, J. D.
MCGRATH, Frederick James
MCKAY, Colin
MCLEAN, Robert
MACRAE, Herbert Tweddle
MADIN, Carl Lionel
MAHAJAN, K. D.
MARKLAND, Frederick George
MATHEW, George
MICHNA, Tadeusz
MIDDLEMISS, Joseph Watson
MILLIGAN, Owen Page
MUNSCH, Anthony Mark
NICHOLLS, Joseph Thomas
NIGHTINGALE, Peter
NURSE, Colin Frederick
NURSEY, John Richard
ORENSTAIN, Jehuda Leo
OXLEY, Victor John
PALMER, David Ernest
PATTERSON, Robert Alfred
PERINI, Flavio
PILGRIM, Ernest Joseph
PITCHERS, John
PONTIN, Ronald Frederick
POOLE, James John
PRABHU, Sudhakar Shrivang
RAWSON, Morris
RICHARDSON, Albert
RICKETTS, Daniel John
ROBINSON, Frank Leonard
ROBINSON, George Leslie
ROBINSON, Michael Douglas
SANDILANDS, Brian Sidney
SATHE, R. M.
SEN GUPTA, Pranab Kumar
SETT, Deb Kumar
SLADE, Harry Jerrold
SMITH, John Frank McLaren
SPICER, Douglas Aubrey
STIEFEL, John Emil
STONE, Peter Albert
SYMES, Ronald Clive
TAYLOR, Eric Henry Frank
THOMSON, John Stuart
TOBUTT, David Cooper
TRUMP, Vernon Henry
TURNBULL, James Neil
TURNER, Frank Herbert
WALKER, Derek
WALLACE, Reginald Rutherford
WEISE, Milton Ludlow
WELSH, John Sturgeon
WESTON, Paul Anchorage
WHITE, Keith Christopher
WHITE, Stanley Francis
WHITING, David Stanley
WILIMOWSKI, Zbigniew Marian
WILSON, Frederick
WILSON, Norman Angus
WOOD, Robert Francis
YOUNG, James
ZEEGEN, Alan Stanley

EXAMINATIONS, JULY, 1961

The Examinations of the Institution will next be held in the United Kingdom and Overseas on the 11th and 12th July, 1961 (Graduateship), and the 13th and 14th July, 1961 (Associate-Membership).

CHANGE OF TELEPHONE NUMBER

The telephone number of the Institution has been changed to BELgravia 4535 (3 lines).

YEAR BOOK AND LIST OF MEMBERS

The Year Book and List of Members for 1961 will go to press in July, for publication in October, when a copy will be sent to all members.

Members are requested to inform the Secretary of any alterations in titles, degrees or addresses, which have not already been notified, by June 24th, in order that such amendments may be included in the new edition.

COMMONWEALTH TECHNICAL TRAINING WEEK

The Institution is staging an exhibition of photographs, models and drawings illustrating the profession of Structural Engineering from 29th May to 2nd June, at 11 Upper Belgrave Street, London, S.W.1.

The exhibition will be open daily from 10 a.m. to 12 noon and from 2 p.m. to 8 p.m. Members of the Institution will be available throughout to answer questions regarding training for the profession and prospects.

During the mornings of Monday, 29th May, Wednesday, 31st May, and Friday, 2nd June, coaches will be provided to take those interested to visit outstanding structures under construction such as Hammersmith Flyover, the Royal College of Arts, and some of the new high buildings.

During the afternoons of these days illustrated talks will be given on various aspects of Structural Engineering and on the Tuesday and Thursday there will be film shows.

It is hoped that members and their friends who are able to do so will visit the exhibition, particularly between 6 and 8 o'clock each evening.

DRURY MEDAL AWARD

The alternative subjects for this eighth competition are a pipe-bridge and a petrol service station.

Graduates and Students of the Institution not over 27 years of age are invited to apply for full details to the Secretary, envelope to be marked at the top left-hand corner 'Drury Medal Award.'

The general conditions of the competition are as follows :—

(a) The competition shall be for Graduates and Students of not more than 27 years of age.

(b) The subjects of the competition will be designs of a structural character, that is to say, involving structural design rather than planning.

(c) The subjects of design and the conditions shall be prepared and issued biennially.

(d) A Jury shall be appointed to examine the work submitted and to interview candidates if found necessary.

(e) In order to ensure that the design submitted is the unaided work of the competitor, the drawings, calculations, etc., submitted shall be endorsed by the candidate: "I declare that the work I hereby submit is my own unaided work." The declaration shall be signed by the competitor, and be either countersigned by a corporate member, or be certified as made before a Justice of the Peace, or a Commissioner for Oaths.

Branch Notices

LANCASHIRE AND CHESHIRE BRANCH

MERSEYSIDE PANEL

The Annual Dinner-Dance will be held at the Carlton Club, Eberle Street, Liverpool, on Friday, 12th May, 1961.

Joint Hon. Secretaries: Wm. Watts, M.I.Struct.E., A.M.I.C.E., 11, Newchurch Lane, Culcheth, Nr. Warrington, Lancs., and M. D. Woods, A.M.I.Struct.E., 8, Dennison Road, Cheadle Hulme, Cheshire.

MIDLAND COUNTIES BRANCH

Hon. Secretary: S. M. Cooper, M.I.Struct.E., 'Applegarth,' 56, Hyperion Road, Stourton, Stourbridge, Worcs.

GRADUATES' AND STUDENTS' SECTION

Hon. Secretary: H. T. Dodd, Shepherd's Cottage, Grove Lane, Wishaw, Sutton Coldfield, Warwicks.

NORTHERN COUNTIES BRANCH

Hon. Secretary: P. D. Newton, B.Sc.(Eng.), M.I.Struct.E., A.M.I.C.E., 6, Cornfield Road, Linthorpe, Middlesbrough, Yorks.

NORTHERN IRELAND BRANCH

Hon. Secretary: L. Clements, A.M.I.Struct.E., A.M.I.C.E., A.M.I.Mun.E., 3, Kingswood Park, Cherryvalley, Belfast, 5.

SCOTTISH BRANCH

Hon. Secretary: W. Shearer Smith, M.I.Struct.E., A.M.I.C.E., c/o The Royal College of Science and Technology, George Street, Glasgow, C.1.

SOUTHERN BRANCH

Hon. Secretary: A. P. K. Tate, B.Sc., A.M.I.Struct.E., Department of Civil Engineering, The University, Southampton.

SOUTH-WESTERN COUNTIES SECTION

Hon. Secretary: C. J. Woodrow, J.P., 'Elstow,' Hartley Park Villas, Mannamead, Plymouth, Devon.

WALES AND MONMOUTHSHIRE BRANCH

Hon. Secretary: W. D. Hollyman, A.M.I.Struct.E., 41, Greenfield Avenue, Dinas Powis, Glam.

WESTERN COUNTIES BRANCH

Hon. Secretary: A. C. Hughes, M.Eng., M.I.Struct.E., A.M.I.C.E., 21, Great Brockeridge, Bristol, 9.

YORKSHIRE BRANCH

Hon. Secretary: W. B. Stock, A.M.I.Struct.E., 34, Hobart Road, Dewsbury, Yorks.

UNION OF SOUTH AFRICA BRANCH

Hon. Secretary: E. B. Kretzchmar, A.M.I.Struct.E., P.O. Box 3306, Johannesburg, South Africa.

Natal Section Hon. Secretary: J. C. Panton, A.M.I.Struct.E., A.M.I.C.E., c/o Dorman Long (Africa) Ltd., P.O. Box 932, Durban.

Cape Section Hon. Secretary: R. F. Norris, A.M.I.Struct.E., African Guarantee Building, 8, St. George's Street, Cape Town.

EAST AFRICA SECTION

Hon. Secretary: K. C. Davey, A.M.I.Struct.E., P.O. Box 30079, Nairobi, Kenya.

SINGAPORE AND FEDERATION OF MALAYA SECTION

Hon. Secretary: J. R. M. MacIntyre, A.M.I.Struct.E., c/o Redpath, Brown & Co. Ltd., P.O. Box 64, Singapore.

NIGERIAN SECTION

Hon. Secretary: A. Brimer, M.I.Struct.E., Brimer Andrews & Nachshen, Private Mail Bag 2295, Lagos, Nigeria.

AUCKLAND (NEW ZEALAND) SECTION
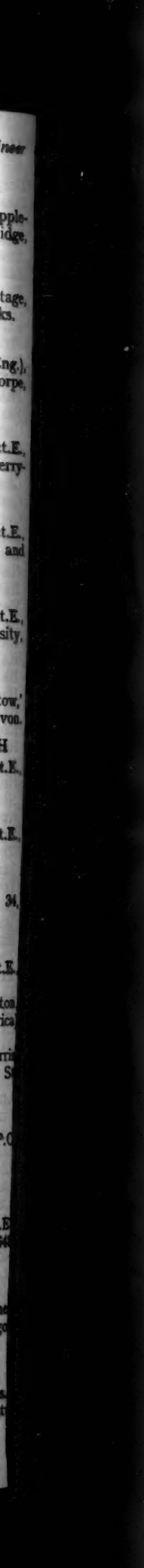
Hon. Secretary: A. Donald, B.Sc.(Hons.), A.M.I.Struct.E., 122, Matipo Road, Te Atatu, Auckland, New Zealand.